SISSA - SCUOLA
INTERNAZIONALE
SUPERIORE
DI STUDI AVANZATI
TRIESTE
Strada Costiera 11

ISAS - INTERNATIONAL SCHOOL FOR ADVANCED STUDIES

THESIS FOR THE ATTAINMENT OF THE TITLE OF

"DOCTOR PHILOSPHIAE"

THEORY OF SPIN EFFECTS IN ELECTRON - ELECTRON SCATTERING IN METALS

==========

Candidate:

Jerzy GLAZER

Supervisor:

Prof. Erio TOSATTI

Section: Physics of Condensed Matter

1984 TRIESTE

CONTENTS

1. INTRODUCTION

The electronic structure determines crucially the properties of metals. One of the most important methods to study them is electron emission from metal surfaces, which may be induced by e.g. high temperatures, strong electric fields, irradiation by energetic photons or by charged particles. In this thesis work we study theoretically the latter process, where electrons are injected, and outgoing electrons are detected. The first evidence for electron emission from metals, induced by electron bombardement , was found in 1902 by Austin and Starke [1] . Since that time a large number of experiments has been performed [2] . The discovery of electron spin and its description by Dirac [3] as a necessary consequence of the principle of relativity was a milestone of physics of course, but in particular initiated the study of the magnetic properties of metals . In 1930 Pauli calculated the spin susceptibility of the free electron gas [4] , and in 1938 Stoner [5] gave the explanation of ferromagnetism in Ni within the band model as a consequence of the exchange interaction between the parallel-spin electrons.

The experimental studies with spin analysis of electrons in metals were, however, not developing very fast. The main reason were the lack of intense sources of polarized electrons and the lack of efficient spin analyzers. Due to the uncertainity principle, together with the Lorentz force , the flux of unpolarized electrons cannot be split into "up" and "down" beams in Stern-Gerlach ty

pe of experiment [6] ; the resulting separation would be always smaller then the wavelenght of the electrons from the beams. In order to detect the spin -orientation the effect of spin-orbit coupling in elastic Coulomb scattering of electrons on heavy atoms, discovered theoretically by Mott in 1929 (see Ref.7), is used up to now. The Mott detector is conceptually simple but the drop in the intensity of electron beam after spin segregation is of several orders of magnitude, which makes measurements quite difficult. It was only in the late sixties that H.C.Siegmann and coworkers in Zürich [8] first detected the spin-polarization of electrons photoemitted from Gd. It took then another ten years for the first observation of electron spin polarization in photoemission from a ferromagnet to be reported [9].

In electron energy loss spectroscopy (EELS) the primary electron (PE) beam is directed on the sample and intensity, energy (and eventually direction) of outgoing electrons are measured. This method has been proven valuable for the investigation of electronic structure of solids [10]. The spin-analyzed version of EELS is called spin polarized electron energy loss spectroscopy (SPEELS). Here,a spin-polarized PE beam is used, or alternatively the spin orientation of the outgoing electrons is detected. This technique has emerged recently, but it has already shown its power. Since the electrons are "marked" by their spin orientation one can detect the electron exchange process which involves spin - flip. The most recent success of this technique is represented by the experiments of Hopster et al. [11] and Kirschner

et al. [12] who detected the spin-flip excitations across the ferromagnetic Stoner gap in Fe [11] and Ni [12].
An earlier, and not less important finding realised with this technique concerned the energy-resolved measurements of spin-polarized secondary electron emitted (SPSEE) from a ferromagnetic material [13]. The secondary electrons (SE), or shortly secondaries, are produced in a cascade process with many individual energy losses processes and also many electrons involved. The SE intensity is relatively large, comparable or larger than the intensity of PE's [2]. This feature is of course desiderable for spin-orientation detection for the reasons mentioned above. In contrast, in SPEELS experiments, where only relatively small losses (compared to the primary energy) are measured, electrons are scattered inelastically only once. This is of course easier to describe theoretically. However, the experimental intensities are at least two orders of magnitude smaller than those of secondaries.

The most puzzling finding in the SPSEE experiments was the large polarization enhancement of low energy secondaries [14-17]. The secondaries of lowest energy, i.e. 0-5eV, show polarizations almost twice as large as the bulk polarization of the ferromagnet they are emitted from. The effect has been found in photo-generated secondary cascades in Fe and Co [14] and in Ni [15], and for electron-generated secondaries emitted from iron-based ferromagnetic glasses [16,17] with PE's used.

The initial motivation for the present thesis work was to explain this polarization enhancement effect.

At the beginning we were trying to employ the simple model of a ferromagnetic metal consisting of two spin-split parabolic bands introduced by Yin & Tosatti [18]. Those early attempts, while giving us fresh understanding of SPSEE, failed totally to describe properly polarization enhancement [19]. This left us with an alternative: a) the enhancement had to do with the d-bands, which were left out in Yin & Tosatti's model, b) the enhancement had another origin, e.g., it was a surface effect. At this point, the results of Hopster et al. became available, showing how strongly spin-polarizing a single exchange event envolving the d-bands could be. We then produced a model which is again the Yin-Tosatti model but enriched with features mimicking the d-bands [20]. This model successfully explained the SPEELS results of Hopster et al., but also turns out to be the basic ingredient for a very satisfactory theory of spin-polarized secondaries.
We end up finally with a coherent picture of single (SPEELS) and multiple (SPSEE) inelastic scattering of electrons in ferromagnets described essentially in terms of Stoner excitations. The empty minority states above the Fermi energy are essential for those excitations. We have found them also to be important for the spin dependence of the inelastic-mean-free-path (InMFP) in the ferromagnets. The effect is strongly energy dependent, and, if confirmed, is of particular importance for the interpretation of the results of spin-polarised electron emission from ferromagnets.

We have also studied the spin effects in the electron-paramagnet scattering. The collision between two free

electrons , called Møller scattering [6] , takes place in the singlet or triplet state with scattering amplitude depending on the electrons spins [6,7]. It allows, the detection of the spin-flip electron-exchange process, once again, if electrons spins are observed. We discuss that possibility for the electron scattered on the Fermi sea of the paramagnetic metal electrons. The simple form and the physical content of the results we have obtained are quite appealing.

This thesis is organised as follows:
in Section 2 we present our model of a ferromagnetic metal and we calculate spin-dependent single inelastic scattering rates. The comparison with experimental SPEELS results [11] is also made. In Section 3 we describe two methods for calculation the secondary polarization in SPSEE : the rate equation approach and computer simulation. This part of the work is a subject of joint theoretical-experimental paper [17]. In the Appendix (placed at the end) we solve analytically simplified version of the rate equations , showing transparently the mechanism of polarization growth with electron energy decay. At the end of Section 3 we describe computer simulation results of SPSEE for a ferromagnet with spatial variation of the magnetization. In Section 4 we give some predictions for future experiments with spin polarized PE beam and spin analyzed scattered electron detection from a free-electron-like paramagnet. This a direct application of the earlier work by Yin & Tosatti. We found that this type of measurement should reveal some important information about electron-electron (e-e) interaction in metals, which could soon be verified experimentally.

tion soon. Section 5 deals with spin dependence of the InMFP of electrons in ferromagnets a subject of substantial practical importance. We show that for low electron energies this dependence can be very strong.

The SPEELS and spin polarized electron emission (SPEE) from metals is very new, fast growing part of condensed matter physics. It it also of practical importance and is already finding applications to data storage systems [21], and to surface magnetometry [22].

The present work is the first comprehensive theoretical study of SPEELS and of SPSEE from itinerant ferromagnets. We feel, we have gained rather good physical understanding of those phenomena.

2. THE MODEL OF FERROMAGNETIC METAL; INELASTIC SPIN-POLARIZED ELECTRON SCATTERING RATES

As the basic ingredient for further considerations, we need to know the inelastic single scattering amplitudes for a high energy electron in a ferromagnetic metal. These amplitudes were first calculated by Yin and Tosatti [18], using the Born approximation, and the simplest spin-polarized parabolic band model. While such parabolic bands probably provide a representation of the sp bands which is not unreasonable, the model is clearly insufficient for describing a real ferromagnet, unless in addition the d-bands are somehow introduced. A simple way to mimic the d-bands [23,24] without increasing the complexity of the calculation has been devised by Glazer & Tosatti [20]. In their model, plane-wave-like parabolic bands are retained, but the density of (minority) $\downarrow$ and (majority) $\uparrow$ states is selectively enhanced by a factor (1+c) in two narrow energy "windows" $(E_F+\Delta/2-\delta, E_F+\Delta/2+\delta)$ and $(E_F-\Delta/2-\delta, E_F-\Delta/2+\delta)$ respectively. Here, E_F is the Fermi energy, Δ is the exchange splitting, and the two quantities (1+c), "window factor", and 2δ, "window width" are adjustable parameters (see Fig.1). Glazer and Tosatti have shown [20], in particular, that once the free parabolic Green's function is replaced by a modified one

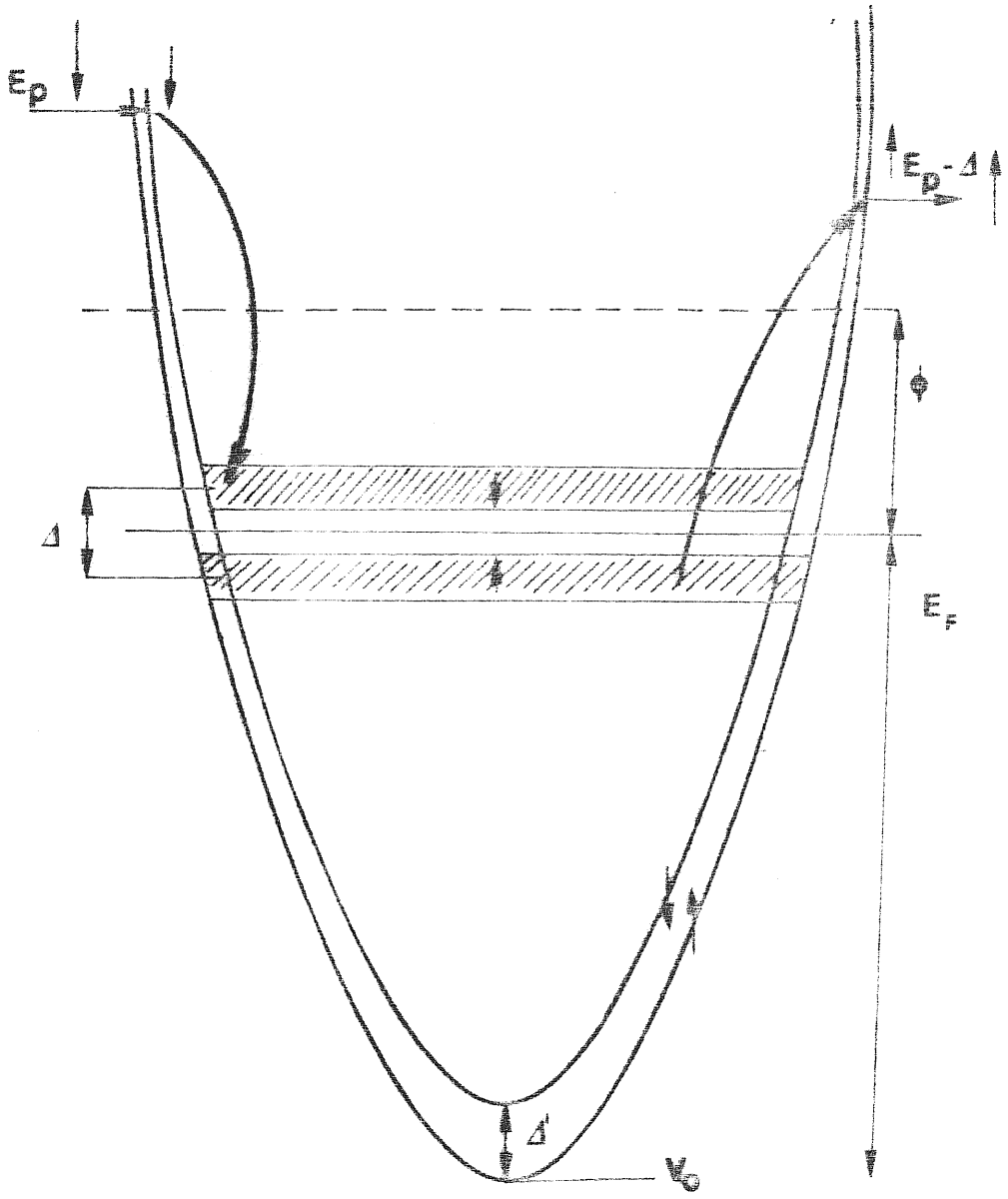

Fig.1.

Schematic band model used in this calculations. The exchange process by which an incoming $(E_p, \downarrow)$ electron is scattered into $(E_p - \omega, \uparrow)$ with creation of a Stoner pair in the d-band is also shown.

$$G^{e,h}(\epsilon, k\sigma) = \frac{1 + c\theta^{W}_{k\sigma}}{\epsilon - \epsilon_{k\sigma} \pm i0^{+}}, \qquad (1)$$

(where $\theta^{W}_{k\sigma}$ is unity when $\epsilon_{k\sigma}$ falls inside a window, and zero otherwise) then the spin-polarized electron energy-loss cross sections of real itinerant ferromagnet such as $Fe_{82}B_{12}S_{6}$ are very well reproduced. Specifically, the band dispersion taken is

$$\epsilon_{k\uparrow} = k^2/2m \qquad (2)$$

$$\epsilon_{k\downarrow} = k^2/2m + \Delta' ,$$

where is an "sp" exchange splitting (not to be confused with the d-band exchange splitting $\sim$2eV). Parameters that were found to reproduce the situation of $Fe_{82}B_{12}Si_{6}$ were c=3.5, δ=0.6 eV, Δ=2.2 eV, Δ'=0.5 eV. For different Fe-based glasses, studied below, we need to adjust only the value of c, keeping other parameters constaht.

The density of states for a given energy is proportional to the imaginary part of the Green's function. Thus, we have for majority $n^{\uparrow}$ and minority $n^{\downarrow}$ spin densities :

$$n^{\uparrow} = \frac{(2m)^{3/2}}{(2\pi)^2} \int_0^{E_F} d\epsilon\, \epsilon^{1/2} \left(1 + c\theta^{W}_{k\uparrow[\epsilon]}\right), \qquad (3a)$$

$$n^{\downarrow} = \frac{(2m)^{3/2}}{(2\pi)^2} \int^{E_F} d\epsilon\, \epsilon^{1/2} \qquad (3b)$$

Note that $\Theta^{W}_{k\sigma}$ is not present in Eq. 3b, since our $d^{\uparrow}$-band window lies above E_F.

Defining the bulk polarization P_b as $P_b=(n^{\uparrow}-n^{\downarrow})/n$ (where $n=n^{\uparrow}+n^{\downarrow}$ is the total density of conduction electrons) we can adjust via Eqs.3 a,b the parameter c to the given value of P_b.

We shall denote by $R^{\uparrow\downarrow}(E,\omega)$ the probability per energy and per unit time that the incoming spin-up electron , of energy E, will,by a single scattering event, lose energy ω and flip to spin-down, and by $R^{\uparrow\uparrow}(E,\omega)$ the same process without spin-flip. Similarly, we call $R^{\downarrow\uparrow}(E,\omega)$, $R^{\downarrow\downarrow}(E,\omega)$ the same quantities for an incoming spin-down electron. The energy E is measured with respect to the bottom of spin-up energy band, so that kinetic energy

$$E_k = E - V_o \qquad (4)$$

where the inner potential V_o is related to the Fermi energy E_f through the work function: $V_o=E_F+\phi$.
We put $V_o=15$ eV and $\phi=4.3$eV.

The scattering rate $R^{\uparrow\downarrow}$ of electron from the state $E(p),\vec{p}\uparrow$ to the final state $E(p)-\omega$, $(\vec{p}-\vec{q})\downarrow$ with momentum transfer $\vec{q}$ and energy transfer ω (see Fig.2 and Ref.25) is proportional in lowest-order perturbation theory to the imaginary part of the forward scattering amplitude:

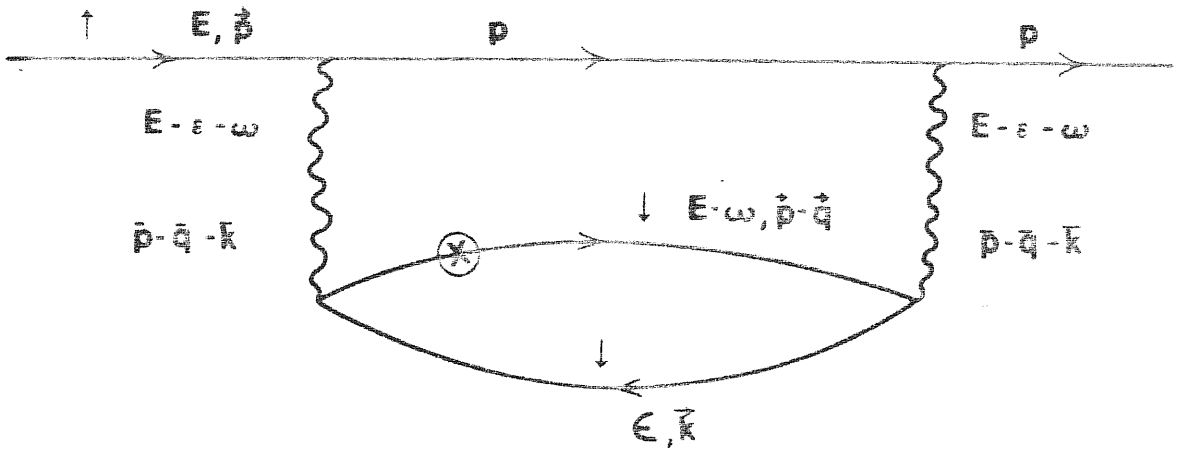

Fig.2

Diagram for the exchange spin-flip process for an incoming spin-up electron. Spin-down electron from initial $\epsilon, \vec{k}^{\downarrow}$ state is excited to $E-\omega, (\vec{p}-\vec{q})^{\downarrow}$ state leaving the hole behind. The cross indicates observed electron.

$$R^{\uparrow\downarrow}(E;q,\omega) = -\frac{2}{\pi}\,\mathrm{Im}\Big[\int\frac{d^3k}{(2\pi)^3}\int\frac{d\epsilon}{2\pi}\times$$
$$\times|V(\vec{p}-\vec{q}-\vec{k})|^2 G^e(E-\omega,(p-q)^{\downarrow})\times$$
$$\times G^e(\epsilon+\omega,(\vec{q}+\vec{k})^{\uparrow})\,G^h(\epsilon,k^{\downarrow})\Big]\,. \qquad (5)$$

As shown in Fig.2 the electron spin is conserved along the electron propagation line, since in the absence of spin-orbit interaction an electron spin cannot be flipped without exchange.

The interaction between electrons is taken to be a statically screened Coulomb potential:

$$V(q) = \frac{4\pi e^2}{(q^2+q_{FT}^2)\Omega}\,, \qquad (6)$$

where q_{FT} is the Thomas-Fermi screening wave vector given by $q_{FT} = (6\pi ne^2/E_F)^{1/2}$, e is the electron charge and Ω is a normalisation volume. The rationale for this choice has beeh discussed in Ref.18 and is roughly as follows. A true lowest order scattering theory would imply in Eq.5 a bare Coulomb interaction $|V(q)| = (4\pi e^2/q^2\Omega)^2$. Full summation of the RPA bubble series would instead yield $|V(q,\omega)|^2 = (4\pi e^2/q^2\Omega)^2\,\varepsilon_{RPA}^{-1}(q,\omega)$, where ε_{RPA} is the q and ω dependent dielectric function. This expression is more accurate - in particular it does take into account excitation of plasmons. However, it has disadvantages for a practical calculations, in that it depends simultaneously and not too simply on both q and ω.

A statically screened form like (6) is less accurate but not too unrealistic, except for ω close to plasmon frequencies. The plasmon oscillator strength is, shifted, with this replacement, from $\omega \sim \omega_p$ to $\omega \sim E_F$, i.e. to electron-hole (e-h) pairs. For our purpose, this is good enough on two accounts: (i) spin - polarization from plasmon scattering is believed to be insignificant[26], (ii) for densities such as those of Fe ω_p and E_F are numerically not very different.

We shall deal here in detail with q-integrated rates only, as many present-day experiments have no momentum transfer selection.

The non - flip $R^{\uparrow\uparrow}(E,\omega)$ scattering rate is a sum of two terms:

$$R^{\uparrow\uparrow}(E,\omega) = R_{\downarrow}^{\uparrow\uparrow}(E,\omega) + R_{\uparrow}^{\uparrow\uparrow}(E,\omega) \qquad (7)$$

The partial rate $R_{\downarrow}^{\uparrow\uparrow}(E,\omega)$ consists of a single contribution, (very similar to Eg.5, once integrated over q).

$$R_{\downarrow}^{\uparrow\uparrow}(E,\omega) = -\frac{2}{\pi}\,\mathrm{Im}\left[\int\frac{d^3q}{(2\pi)^3}\int\frac{d^3k}{(2\pi)^3}\int\frac{d\epsilon}{2\pi}\times\right.$$
$$\times |V(\vec{q})|^2\, G^e\left(E-\omega,(p-q)^{\uparrow}\right) G^e\left(\epsilon+\omega,(\vec{q}+\vec{k})^{\downarrow}\right)\times$$
$$\left.\times\, G^h(\epsilon,k^{\downarrow})\right]. \qquad (8)$$

The other partial rate $R_{\uparrow}^{\uparrow\uparrow}(E,\omega)$ is made up of several contributions, because of particle indistinguishability

$$R_{\downarrow}^{\uparrow\uparrow}(E,\omega) = -\frac{2}{\pi}\,\mathrm{Im}\Big[\int\frac{d^3q_{\downarrow}}{(2\pi)^3}\int\frac{d^3k}{(2\pi)^3}\int\frac{d\epsilon}{2\pi}\times$$
$$\times G^{e}(E-\omega,(\vec{p}-\vec{q}_{\downarrow})^{\uparrow})\,G^{e}(\epsilon+\omega,(\vec{q}_{\downarrow}+\vec{k})^{\uparrow})\times$$
$$\times G^{h}(\epsilon,k^{\uparrow})\times\left(|V(q_{\downarrow})|^2+|V(\vec{p}-\vec{q}_{\downarrow}-\vec{k})|^2+\right.$$
$$\left.-2V(q_{\downarrow})V(\vec{p}-\vec{q}_{\downarrow}-\vec{k})\left(1+c\,\theta^{W}_{k\uparrow[\epsilon]}\right)^{-1}\right)\Big]. \qquad (9)$$

The first two terms in Eq.9 represent direct and exchange scattering respectively. The third term (negative) appears naturally if all lowest order diagrams are included and is the quantum - mechanical interference between amplitudes of direct and exchange process [6,7]. The factor $(1+c\,\theta^{W}_{k\uparrow})^{-1}$ in that term cancels the enhancement $(1+c\,\theta^{W}_{k\downarrow})$ of Eq. (1) for these terms only. The idea is that exchange interference term should be negligible for states belonging to different shells.

Four out of the seven integrations inherent in Eq.8 & 9 can be done analytically. The remaining three are left for numerical calculations.

The quantities $R^{\downarrow\uparrow}(E,\omega)$ and $R^{\downarrow\downarrow}(E,\omega)$ are computed in the same way, namely:

$$R^{\downarrow\uparrow}(E,\omega) = -\frac{2}{\pi}\,\mathrm{Im}\Big[\int\frac{d^3k\,d^3q_{\downarrow}\,d\epsilon}{(2\pi)^7}|V(\vec{p}-\vec{q}_{\downarrow}-\vec{k})|^2\times$$
$$\times G^{e}(E-\omega,(\vec{p}-\vec{q}_{\downarrow})^{\uparrow})\,G^{e}(\epsilon+\omega,(\vec{q}_{\downarrow}+\vec{k})^{\downarrow})\times$$
$$\times G^{h}(\epsilon,k^{\uparrow})\Big], \qquad (10)$$

and:

$$R^{\downarrow\downarrow}(E,\omega) = R_{\uparrow}^{\downarrow\downarrow}(E,\omega) + R_{\downarrow}^{\downarrow\downarrow}(E,\omega), \tag{11}$$

where:

$$R_{\uparrow}^{\downarrow\downarrow}(E,\omega) = -\frac{2}{\pi}\,\mathrm{Im}\left[\int \frac{d^3q\,d^3k\,d\epsilon}{(2\pi)^7}\,|V(\vec{q}_{\downarrow})|^2 \times \right. \tag{12a}$$
$$\left. \times\, G^e(E-\omega,(\vec{p}-\vec{q}_{\downarrow})^{\downarrow})\, G^e(\epsilon+\omega,(\vec{q}_{\downarrow}+\vec{k})^{\uparrow})\, G^h(\epsilon,k^{\uparrow})\right],$$

$$R_{\downarrow}^{\downarrow\downarrow}(E,\omega) = -\frac{2}{\pi}\,\mathrm{Im}\left[\int \frac{d^3q\,d^3k\,d\epsilon}{(2\pi)^7}\, G^e(E-\omega,(\vec{p}-\vec{q}_{\downarrow})^{\downarrow}) \times \right. \tag{12b}$$
$$\times\, G^e(\epsilon+\omega,(\vec{q}_{\downarrow}+\vec{k})^{\downarrow})\, G^h(\epsilon,k^{\downarrow}) \times \left(|V(\vec{q}_{\downarrow})|^2 + \right.$$
$$+|V(\vec{p}-\vec{q}_{\downarrow}-\vec{k})|^2 - 2V(q_{\downarrow})V(\vec{p}-\vec{q}_{\downarrow}-\vec{k}) \times (1+c\theta^{W}_{(\vec{p}-\vec{q}_{\downarrow})^{\downarrow}})^{-1} \times$$
$$\left.\left. \times\,(1+c\theta^{W}_{(\vec{q}+\vec{k})^{\downarrow}})^{-1}\right)\right].$$

We have carried out calculations as a function of E and ω that are required in further discussion. As an example we display in Fig.3 the results for c=2 (P_B=22%) for up and down-spin electron with initial energy 10 eV above the vacuum level.

The most striking features in Fig.3 are the chimney-like structures for the $R^{\downarrow\downarrow}$ and $R^{\uparrow\downarrow}$ functions. They are both the consequences of the abrupt square shape we have assumed for the $d^{\downarrow}$-band window. One can vary the shape of the $\theta^{W}_{k\sigma}$ functions, e.g. by making it smooth, but this would not change the most important physical features of the model.

The spin-flip scattering $R^{\uparrow\downarrow}$ (via the exchange process) for spin-up electron is enhanced when the excited

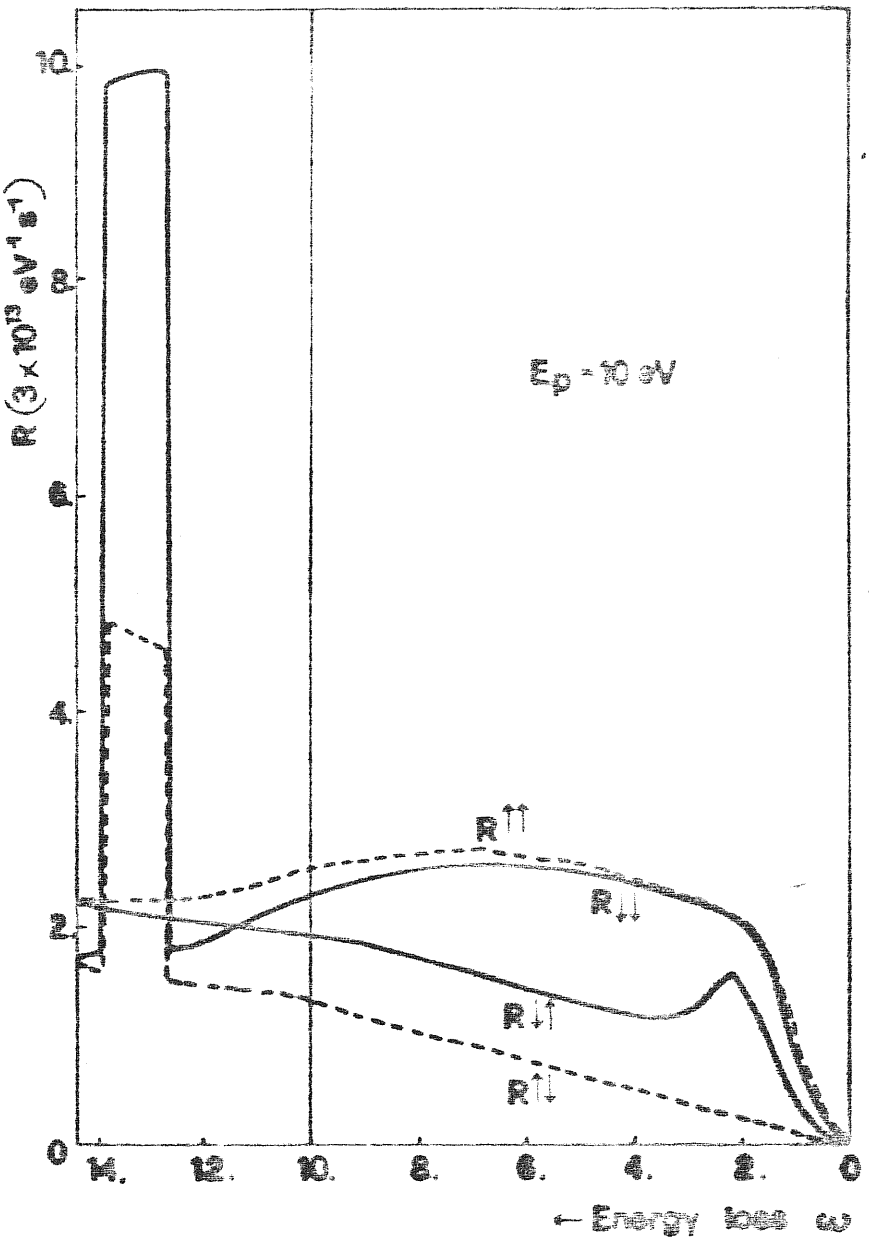

Fig.3

Energy loss rates for spin-up (down) electron with primary enrgy E_p=10 eV measured with respect to vacuum level V_o, as a function of energy loss ω. Vertical line marks the vacumm level.

spin-down electron falls into the $d^{\downarrow}$-band, the same happens for non-flip scattering for spin-down electrons. In the latter case however both processes are possible: Direct (when the scattered electron falls into the $d^{\downarrow}$--band) and exchange scattering (when the spin-down electron excited from below E_F falls into the $d^{\downarrow}$-band). This is the reason why $R^{\downarrow\downarrow}(E,\omega)$ is much larger than $R^{\uparrow\downarrow}(E,\omega)$ when $E-\omega$ is within the $d^{\downarrow}$-band.

The maximum for ω =2.2 eV for $R^{\downarrow\uparrow}(E,\omega)$ reflects the scattering process where both $d^{\uparrow}$ and $d^{\downarrow}$ bands are involved: a spin-down electron falls into the $d^{\downarrow}$-band exciting a spin-up electron from the $d^{\uparrow}$-band with energy loss ω close to the d-band exchange splitting Δ[20] (see Fig.1) . This amounts just to creating a Stoner excitation in the metal. Since both filled and empty d -bands contribute to the $R^{\downarrow\uparrow}$ scattering rate , the maximum of $R^{\downarrow\uparrow}$ has a triangular shape due to the self-convolution of the d-density. On the other hand no Stoner excitation can be created by an up spin electron. As a result $R^{\uparrow\downarrow}$ is much smaller then $R^{\downarrow\uparrow}$ for $\omega \sim \Delta$. The effect of this asymmetry has been observed experimentally in spin-polarized electron energy loss spectroscopy (SPEELS) in Fe - based ferromagnetic metalic glass [11] and in Ni [12] .
The SPEELS polarization measured in ref.11 is, in the simplest scheme, equal to the "outgoing asymmetry parameter"

$$A_{OUT_\omega}(E_p)=\frac{\left(R^{\uparrow\uparrow}(E_p,\omega)+R^{\downarrow\uparrow}(E_p,\omega)\right)-\left(R^{\downarrow\downarrow}(E_p,\omega)+R^{\uparrow\downarrow}(E_p,\omega)\right)}{\left(R^{\uparrow\uparrow}(E_p,\omega)+R^{\downarrow\uparrow}(E_p,\omega)\right)+\left(R^{\downarrow\downarrow}(E_p,\omega)+R^{\uparrow\downarrow}(E_p,\omega)\right)}, \qquad (13)$$

where E_p is the kinetic energy of a primary electron. Our result obtained for A_{out} is presented and compared with experiment in Fig.4. The best agreement is obtained by giving the window parameter c a value between 3 and 3.5. The main process contribution to the peak at is that of Fig.1 , involving a Stoner excitation. The magnitude of this peak is found to decrease rapidly for large primary energies E_p , which agrees very well with experiment , as shown in Fig.5, as well as with our physical expectation for an exchange process. No such increase is however reported for E_p between 18 and 5 eV in Ni[11]. The reason for this can probably be traced to band-structure matrix-element effects that are omitted in our simple model, but should be important at low energies.

As a further check on the implications of our mechanism, we can calculate the EELS intensity line shape (not spin-analysed). This is proportional to

$$R(E_p,\omega)=R^{\uparrow\uparrow}(E_p,\omega)+R^{\downarrow\downarrow}(E_p,\omega)+R^{\uparrow\downarrow}(E_p,\omega)+R^{\downarrow\uparrow}(E_p,\omega), \quad (14)$$

which is plotted in Fig.6 for various primary energies. A characteristic d-band shoulder, or hump, is predicted for losses near the exchange splitting $\omega\sim\Delta$. The occurrence of this hump in Fe is currently being investigated in Fe by Rosei and coworkers[27] . The hump height is predicted to be also energy-dependent as in Fig.3. Features reminiscent of those in Fig.4 have been reported by Ibach and Lehwald[28] for Ni. Their interpretation of a direct spin-flip process $d^{\uparrow}\rightarrow d^{\downarrow}$ should probably, in view of our evidence, be revised to an exchange spin-flip as in Fig.1.

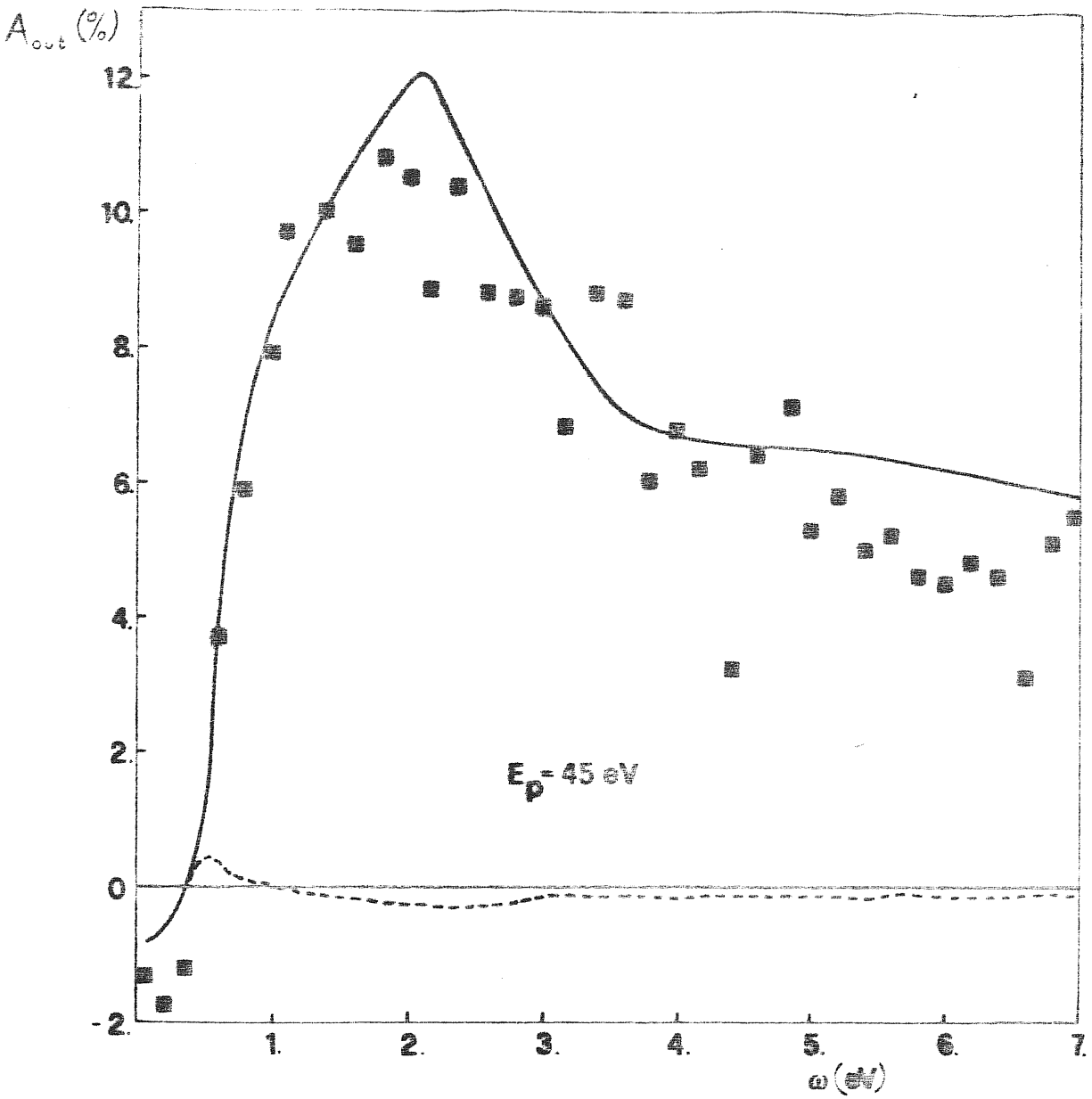

Fig.4

Calculated spin asymmetry A_{out} (Eq.13), without (lower curve, c=0) and with (upper curve) d-bands. A good agreement with experimental data of Ref.11 is achieved as shown, with c=3.5, other parameter chosen so as to approximate the situation for Fe.

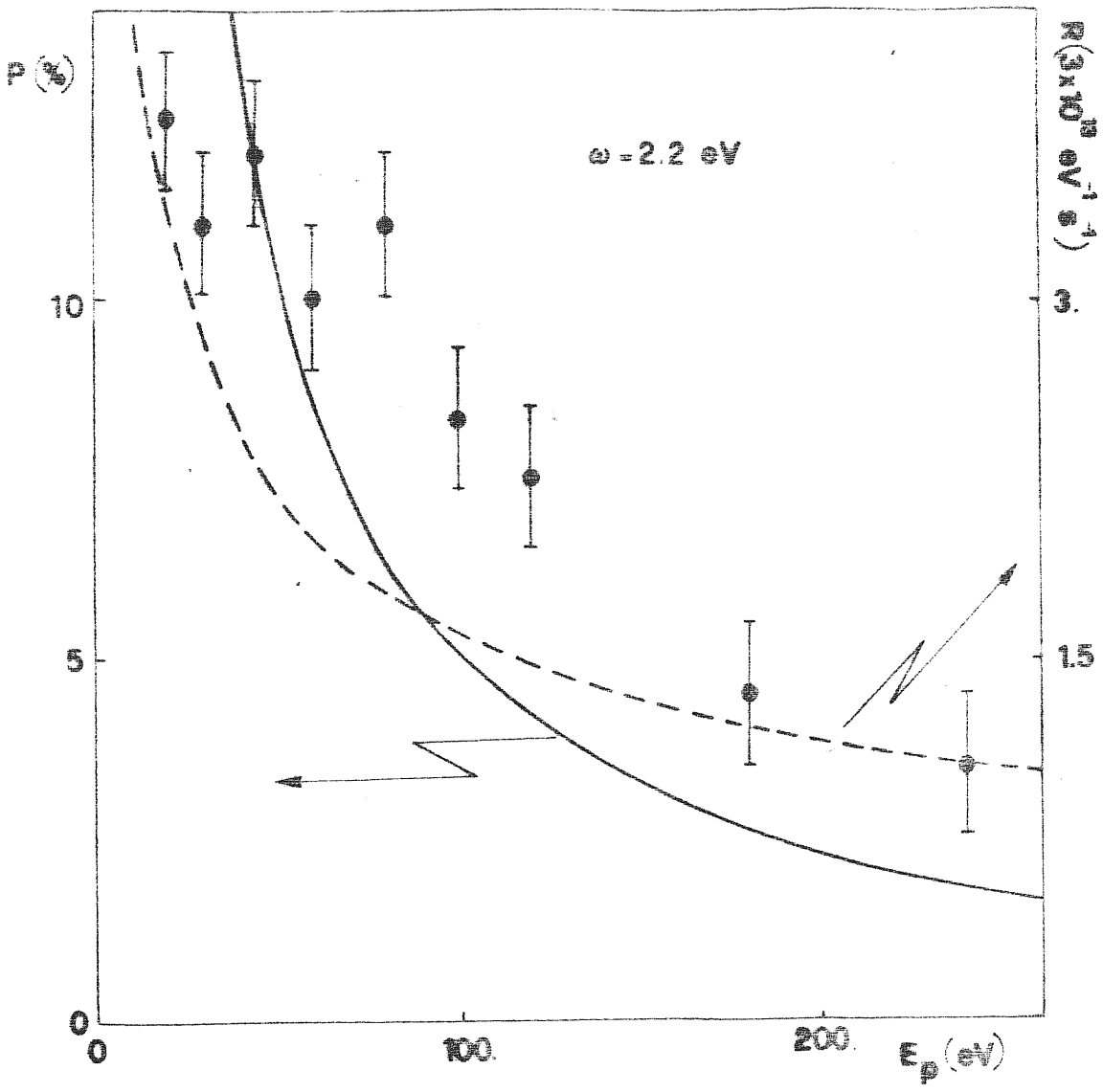

Fig.5

Primary energy dependence of the main polarization peak of Fig.4 (full curve) and of the total intensity hump (Eq.14) of Fig.6 (dashed line). The rapid fall with increasing E_p seen both in theory and experiment (Ref.11) is strong evidence for an exchange process in Fig.1.

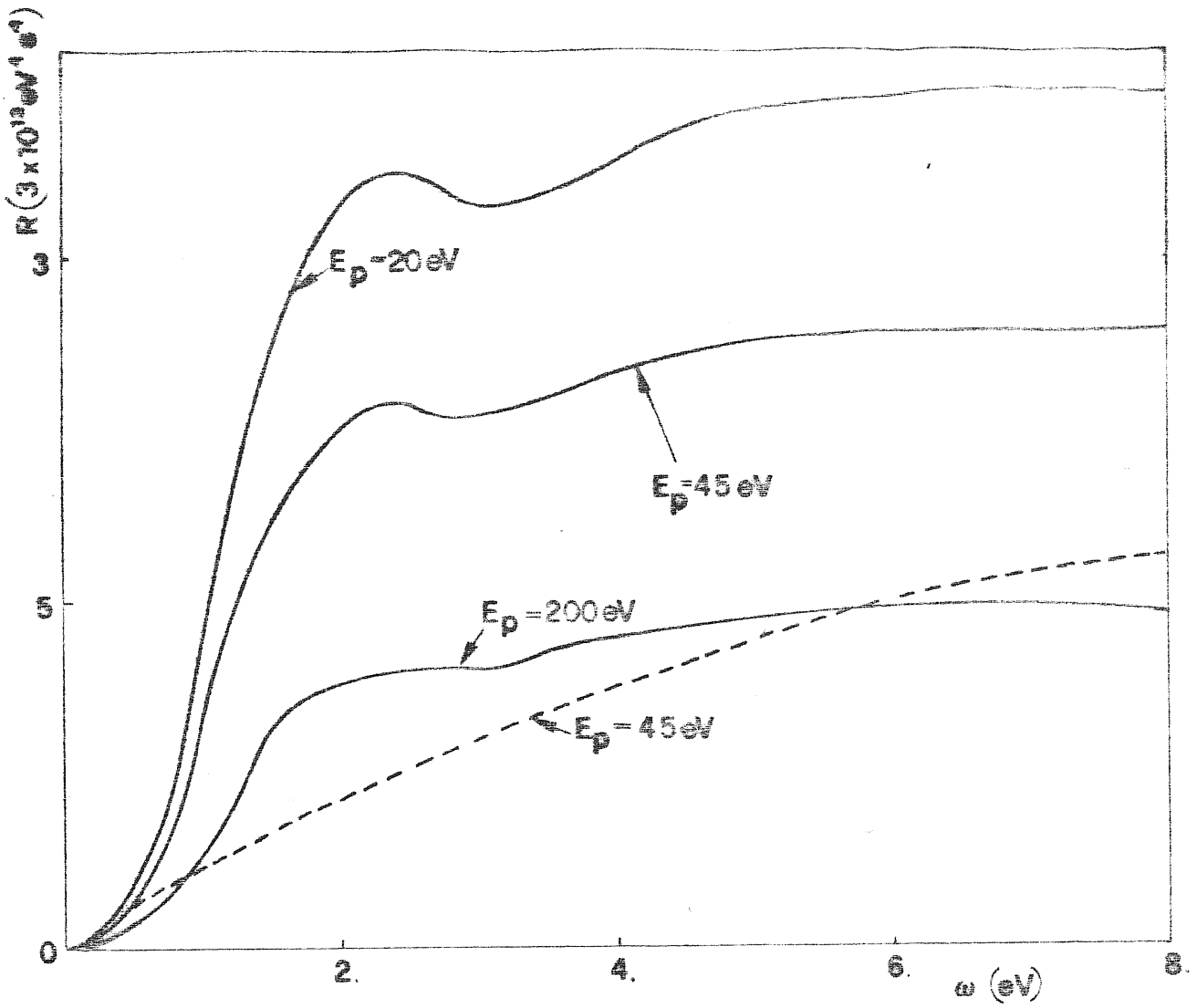

Fig.6

Total EELS (Eq.14) calculated for Fe. Lower curve : no d-bands. Upper curves : with d-bands, for various primary energies. The hump around 2eV reflects the process of Fig.1.

3. FERROMAGNETIC METAL; CASCADE OF SECONDARY ELECTRONS.

When an energetic PE is injected into a metal it will lose its energy mainly via e-h pair creation. The electrons excited above the Fermi level E_F in this process travel through the metal being scattered both elastically (e.g. Bragg-diffracted by the lattice) and inelastically, by giving rise to futher e-h pairs. Some of these electrons eventually leave the metal, crossing its surface. Those electrons which leave after so many inelastic scattering events that their energy is reduced to 10-20 eV or less are the SE.

The theory of secondaries has been developed decades ago [2] and is now well established [29-33]. The spin plarization of SE however has not been discussed theoretically.

As a first guess, the fact that the largest fraction of secondaries is excited out of the valence bands, suggests that their polarization has to be close to the bulk polarization P_b. The experimental findings [14-17] indicated however, quite surprisingly, that the polarization of SE of lowest energy is about twice P_b for ferromagnetic Fe, Ni, and Co. This effect of polarization enhancement has been attributed to the spin-dependent exchange scattering [9,15] and to the increase of minority--electron decay due to the large number of empty minority-

-spin states just above the Fermi level [14,15].

Below we present calculations where both of the above mechanisms contribute to the SE polarization enhancement in a manner that makes them hard to separate. The results are compared with SPSEE experiments performed with ferromagnetic metalic glasses based on iron. Variable Fe concetration gives an ideal opportunity to check the theoretical results with respects to different bulk plarization P_b.

There are two basic steps involved in our spin-polarized calculation of secondaries. The first is the determination of cross-section for a single scattering event (it is already done in Section 2.) The second step is to calculate the polarization of hot electrons excited above E_F. A quantum-mechanical treatment of a large number of scattering events including overall phase coherence is in practice out of the question. It is clear, however, that to some extent such a level of complication is excessive. For increasing electron energies, for example, quantum-mechanical interference between products of scattering amplitudes relative to different events should rapidly become negligible - we have made the approximation that such interferences can in fact be neglected altogether, thereby abandoning scattering amplitudes in favour of cross sections of successive events, assumed to be unrelated.

Within this approximation we have carried out two separate and parallel calculations. The first approach is based on a simple rate equilibrium, of up and down-spins as a function of energy. The corresponding master

equation is constructed and solved numerically . The second approach consists of a computer experiment, where the cascade generated by one fast incoming electron is followed step by step, with probabilities for successive events taken from the microscopic theory of inelastic electron scattering. In this latter approach the geometry of the problem is also included, and a much more detailed study of the properties of the secondary electron cascade in space, energy, and spin is possible.

3.1 Rate Equation Approach.

Suppose a continious flux of primary electrons is being injected into a metal, and thus generates the cascade of hot electrons. All those electrons lose energy by inelastic scattering off other metal electrons. Their final fate is either to decay to Fermi level or to escape from the metal across the surface. After an initial transient regime, a dynamical equilibrium has to be reached where the spin-resolved energy distributions $I^{\uparrow}(E)$, $I^{\downarrow}(E)$ of hot electrons, both inside, and escaping become time-dependent.

We neglect here escape of the electrons altogether or, equivalently, we assume an infinite metal, where the surface is negligible. This makes things much simpler, since then we do not need to worry about: a) the geometry of the problem and b) elastic scattering of the electrons (as long as we can assume that it is spin-independent). We then assume that the energy and spin distribution of SE is the same as the distribution of hot electrons in the metal.

At dynamical equilibrium the number of electrons per unit time which fall, through flip or non-flip inelastic scattering, down, to energy E with spin-up(down) is equal to the number of spin-up (down) electrons with energy E scattered inelastically further down in the same time. One can then write a pair of coupled master equations:

$$\int_0^{E_0-E} d\omega \left[R^{\uparrow\uparrow}(E+\omega,\omega) I^{\uparrow}(E+\omega) + R^{\downarrow\uparrow}(E+\omega,\omega) I^{\downarrow}(E+\omega) \right] =$$

$$= \int_0^{E-E_F} d\omega \left[R^{\uparrow\uparrow}(E,\omega) I^{\uparrow}(E) + R^{\uparrow\downarrow}(E,\omega) I^{\uparrow}(E) \right] , \qquad (15a)$$

$$\int_0^{E_0-E} d\omega \left[R^{\downarrow\downarrow}(E+\omega,\omega) I^{\downarrow}(E+\omega) + R^{\uparrow\downarrow}(E+\omega,\omega) I^{\uparrow}(E+\omega) \right] =$$

$$= \int_0^{E-E_F} d\omega \left[R^{\downarrow\downarrow}(E,\omega) I^{\downarrow}(E) + R^{\downarrow\uparrow}(E,\omega) I^{\downarrow}(E) \right] , \qquad (15b)$$

where E_o is some initial electron energy, e.g., the primary electron energy. On the left side in both equations are the numbers of up (Eq.15a) and down (Eq.15b) electrons falling to the energy E, on the right are the numbers of electrons leaving the states with energy E. We are concerned only with $E > V_o$, i.e. only with electrons which in vacuum would have positive kinetic energy. Note, however that electrons have the possibility to decay into the energy region of width ϕ between the vacuum level V_o and the Fermi energy E_F, hence the integration limit $E-E_F$ on the right-hand side.

Our aim is now to calculate from Eq.15a & b the two unknown functions $I^{\uparrow}(E)$ and $I^{\downarrow}(E)$ for $V_o \leq E \leq E_o$ with boundary conditions $I^{\uparrow}(E_o) = I_o^{\uparrow}$ and $I^{\downarrow}(E_o) = I_o^{\downarrow}$. From $I^{\uparrow}$ and $I^{\downarrow}$ we will eventually calculate the SE

and polarization P :

$$I(E) = I^{\uparrow}(E) + I^{\downarrow}(E) \quad , \tag{16}$$

$$P(E) = \frac{I^{\uparrow}(E) - I^{\downarrow}(E)}{I^{\uparrow}(E) + I^{\downarrow}(E)} \quad . \tag{17}$$

In principle E_o has to be equal to the energy of the PE beam E_p and $P_o = (I^{\uparrow}_o - I^{\downarrow}_o) / (I^{\uparrow}_o + I^{\downarrow}_o)$ ought to be the PE polarization. What we find however is that the intensity and polarization of SE calculated according to Eq.15-17 is practically independent of E_o and P_o if the kinetic energy of PE is higher than 100eV and P_o is between zero and P_b (*). Since the problem is linear, we can also set $I^{\uparrow(\downarrow)}_o = 1$, i.e., we use relative intensities.

The solution of the integral equations 15a and 15b has been done numerically by the iteration (simplified problem can be solved analytically - see Appendix) :

$$I_{n+1}(E) = I^{\uparrow}_n(E) + \int_0^{E_o-E} d\omega \left[R^{\uparrow\uparrow}(E+\omega,\omega) I_n^{\uparrow}(E+\omega) + R^{\downarrow\uparrow}(E+\omega,\omega) I_n^{\downarrow}(E+\omega) \right] - \int_0^{E-E_F} d\omega \left[R^{\uparrow\uparrow}(E,\omega) I_n^{\uparrow}(E) + R^{\uparrow\downarrow}(E,\omega) I_n^{\uparrow}(E) \right] , \tag{18a}$$

---

* Note again that no provision for geometrical factors, and escape depth, etc., is made in the single formulation given in this Section. Due to these, I and P may of course pick up an extra dependence on E_o, P_o as discussed further below.

$$I^{\downarrow}_{n+1}(E) = I^{\downarrow}_{n}(E) + \int_0^{E_0-E} d\omega \left[R^{\downarrow\downarrow}(E+\omega,\omega)\, I_n^{\downarrow}(E+\omega) + R^{\uparrow\downarrow}(E+\omega,\omega)\, I_n^{\uparrow}(E+\omega) \right] \int_0^{E-E_F} d\omega \left[R^{\downarrow\downarrow}(E,\omega) \times I_n^{\downarrow}(E) + R^{\downarrow\uparrow}(E,\omega)\, I^{\downarrow}_n(E) \right], \qquad (18b)$$

where $I^{\uparrow(\downarrow)}_n(E)$ is the spin-up (down) energy distribution function calculated in n-th iteration. For a number of iterations N large enough so that $I^{\uparrow(\downarrow)}_N(E)$ and $I^{\uparrow(\downarrow)}_{N+1}(E)$ become practically independent of N, we can take $I^{\uparrow}_N(E)$ and $I^{\downarrow}_N(E)$ as the solution of Eqs.15 a & b.

We have found $I^{\uparrow}(E)$ and $I^{\downarrow}(E)$ for scattering rates calculated for c=2. ; 1.4 ; .75, corresponding to P_b = 22% ; 19% ; 15% respectively, if $\Delta^{\prime}$ =.5 eV is kept fixed. The detailed discussion of the results is presented in the following subsection. Here we only want to point out that the intensity I of SE we found (see Fig.8 --solid line) obeys an E^{-m} law [31] with m = 2.

3.2 A computer simulation.

As pointed out in the beginning of this Section the neglect of quantum interference effects allows the discussion of the electron cascade in purely classical terms, easily amenable to direct computer simulation. Many cascade studies have been carried out [29-33]. Some of them are based on Monte-Carlo computer simulations [32,33]. The present simulation, though analogous in spirit, has been developed independently. It is simple and unsophisticated, but it contains the important new ingredient of spin selection. An electron is considered a point particle moving in space and time. Each electron above the Fermi level is kept track of independently, with respect to its energy, momentum and spin state. The continous trajectory of an electron is broken into "hops" of length Δl, which is chosen tentatively to be 1Å. At the end of each "hop" the electron with energy E, can suffer inelastic scattering. Now consider what happens for example to a spin-up electron. Inelastic scattering will occur with a probability given by :

$$P = \mathcal{P}^{\uparrow}(E)\,\Delta l / v^{\uparrow}(E) \quad , \tag{19}$$

where $v^{\uparrow}(E) = (2E/m)^{1/2}$ is the velocity of spin-up electrons with energy E (for down-spin : $v^{\downarrow}(E) = (2(E-\Delta')/m)^{1/2}$), while $\mathcal{P}^{\uparrow}(E)$ is a probability per unit time for spin-up electrons with energy E that any inelastic event occurs:

$$\mathcal{P}^{\uparrow}(E)=\int_{0}^{E-E_F} d\omega \left(R^{\uparrow\uparrow}(E,\omega)+R^{\uparrow\downarrow}(E,\omega)\right) . \qquad (20)$$

During the inelastic scattering event a spin - up electron with energy E and momentum $\vec{p}$ loses energy and transfers momentum $\vec{q}$ to the created e-h pair system. After this scattering there are two electrons above Fermi level : one with momentum $\vec{p}-\vec{q}$, another with momentum $\vec{q}+\vec{k}$. The momenta $\vec{q},\vec{k}$ and spins of the electrons have to be chosen with proper probability.

From the discussion of Section 2, the probability $P(\vec{p}^{\uparrow};(\vec{p}-\vec{q})^{\downarrow},(\vec{q}+\vec{k})^{\uparrow})$ that a spin-up electron with momentum $\vec{p}$ (and energy E) produces a spin-up electron with momentum $\vec{p}-\vec{q}$ (and energy $E-\omega$) and a spin-down electron with momentum $\vec{q}+\vec{k}$ is proportional to (all momenta and energies are expressed in terms of p_F and $2E_F$ respectively, where $p^{\uparrow}_F=\sqrt{2mE_F}$) :

$$P(\vec{p}^{\uparrow};(\vec{p}-\vec{q})^{\downarrow},(\vec{q}+\vec{k})^{\uparrow}) \propto \frac{\theta(|\vec{q}+\vec{k}|-1)\,\theta((1-\tfrac{1}{2}\Delta')^{1/2}-k)}{((\vec{p}-\vec{q}-\vec{k})^2+q_{FT}^2}\times$$

$$\times\left(1+c\theta^{W}_{(\vec{p}-\vec{q})^{\downarrow}}\right)\left(1+c\theta^{W}_{(\vec{q}+\vec{k})^{\uparrow}}\right) , \qquad (21)$$

and with the same notation :

$$P(\vec{p}^{\uparrow};(\vec{p}-\vec{q})^{\uparrow},(\vec{q}+\vec{k})^{\downarrow}) \propto \frac{\theta((1-2\Delta')^{1/2}-k)\,\theta(|\vec{q}+\vec{k}|-|1-2\Delta'|^{1/2}))}{(q^2+q_{FT}^2)^2} \times$$

$$\times\left(1+c\theta^{W}_{(\vec{q}+\vec{k})^{\downarrow}}\right) , \qquad (22)$$

$$P(\vec{p}^{\uparrow};(\vec{p}-\vec{q})^{\uparrow},(\vec{q}+\vec{k})^{\uparrow}) \propto \theta(|\vec{q}+\vec{k}|-1)\,\theta(1-k)\times$$

$$\times\left\{\left[\frac{1}{(q^2+q_{FT}^2)^2}+\frac{1}{((\vec{p}-\vec{q}-\vec{k})^2+q_{FT}^2)^2}\right]\left(1+c\theta^{W}_{(\vec{q}+\vec{k})^{\uparrow}}\right)+\right.$$

$$\left.-\frac{2}{(q^2+q_{FT}^2)((\vec{p}-\vec{q}-\vec{k})^2+q_{FT}^2)}\right\} . \qquad (23)$$

Here the θ-functions take care of the Pauli principle. However, the electron at $E-\omega$, $(\vec{p}-\vec{q})^{\uparrow(\downarrow)}$ is automatically above E_F since we consider energy loses with $\omega \leq E - E_F$. Energy conservation requirement adds one more condition for $\vec{q}$ and $\vec{k}$: $\vec{p}\cdot\vec{q} = \vec{q}\cdot\vec{k} + q^2$.

The absence of the enhancement factor $(1 + c\theta_k^W)$ in the negative interference exchange term in the Eq.23 has been discussed in previous Section. Similar formulae to these can be written for scattered spin-down electrons.

After this scattering event, we have two electrons plus a hole, all with well-defined spin and momenta travelling through the metal, exciting eventually other electrons ; In principle this cascade process is infinite and each electron which does not escape out of the surface reaches the Fermi level through repeated inelastic scattering.

As an approximation, we choose to neglect energy loss processes due to inelastic scattering by the hole, and the new e-h pairs thus generated. Since the hole can only lose energy $\omega < E_F$, the chance that it can give rise to an electron with sufficient energy to be relevant as a secondary is finite, but very small.

The only electrons interesting for us are those electrons which have a chance to cross the surface of the metal and be observed as secondaries. Therefore, after inelastic scattering the energies of two electrons are checked and those with energy less than vacuum zero V_o are dropped, since their only fate is to sink to the Fermi sea.

So far, we have not discussed how the geometrical factors enter our simulation. This happens in two ways. The first is that it is necessary for an electron to have a direction very different from the incident electrons , for it to be observed as a secondary. The inelastic processes considered here do actually involve a deflection, but

the probability of a large deflection is very small, even after repeated scattering. It is physically clear that large - angle elastic scattering , for example Bragg scattering in the crystalline case, is crucial in determining large observed yield of secondaries.[35] We shall describe further down the very simple way we use for introducing electron deflection, actually done by elastic scattering. The second is that escape out of the surface has, in the simplest potential step scheme, a certain kinematic dependence upon the angle of incidence of the electron which attempts the escape against the surface. This kinematic restriction has to do chiefly with the parallel momentum conservation - while of course the normal momentum is not conserved, when the electron crosses the surface. We calculate SE yields both with and without this kinematical restriction. The resulting intensities are very similar, except at very low E_k , where electron escape is strongly suppressed by parallel momentum conservation. It is interesting to note that most available data resemble much more the calculation done without kinematical restriction. In our opinion, this could be because the surface of the amorphous material is so imperfect that parallel momentum conservation isirrelevant. Following this reasoning, we conclude, that, while the full escape kinematics should of course be used for an ideally flat surface, the best one can do for a real surface is to ignore it altogether, and assume that each electron that hits the surface with energy $E > V_o$ will just escape, no matter what angle it forms with the surface.

Elastic scattering is, both in principle and in prac

tice a much more delicate problem to deal with. Calculating its intensity is non trivial [36], requires the use of highly sophisticated codes. Furthermore, elastic scattering is spin-dependent, although the resulting asymmetries are only of the order of a few percent in amorphous Fe [37]. This last fact provides one sole justification for neglecting any spin- polarization arising from elastic scattering. A simple inelastic scattering event will usually be more spin - polarizing than this (see Fig. 4).

There remains the geometrical problem of how to produce, within our computer simulation, the large - angle elastic scattering required to turn electrons out of the sample.

Elastic scattering is crudely replaced in our simulation by a "mirror" which scatters back the electrons. The depth where the "mirror" is placed can be adjusted by fixing the total yield Y of secodaries ($Y = N_{out}/N_{in}$, where N_{in} is a number of PE and N_{out} is a number of SE). Too small and to big mirror depths make Y small since in the first case the cascade of secondaries has not enough space to develop and in the second case electrons have a small chance to reach the surface. We have found a mirror depth of six times the InMFP see Section 5 to be the most realistic. In that case the yield Y for PE with primary energy E_p (measured with respect to the vacuum level) of 400 eV is $Y \approx 1.6$ which seems reasonable compared with experimental data [2].

In the simulation the primary energy E_p, the electron angle of incidence (measured with respect to the surface normal) and the bulk polarization P_b (i.e. parameter c)

of the metal are to be chosen at the begining. Each "experiment" consists of repeated injections of one electron with the same momentum $\vec{p}$ and with different spin orientation. As the PE beam in the real experiment is unpolarized- we have injected the same number of up and down electrons. A large number of primaries is needed for each simulation ($\sim 10^5$) in order to achieve reasonably accurate values of yield and polarization of secondaries for kinetic energies below 10 eV.

Data of outgoing electrons are stored. Histograms can than be made, with an one eV as the energy interval. The results are shown in Fig.7 for c = 3.;2.;1.4;0.75 (P_b = 27% , 22% , 19% , 15% respectively). The strong enhancement, with its magnitude depending on P_b , of electron polarization for small kinetic energies is observed.

In Fig.8 we show the SE intensities. The shapes are practically independent of the ferromagnetic glass we used. There is almost absolute agreement between intensities obtained by solving the master equations and by doing the simulation without surface scattering. This is not surprising : In the simulation each secondary electron is produced on the average after about 10 inelastic events with various energy transfers. It seems enough for the system of hot electrons to be very close to the equilibrium distribution as predicted by the master equations. Some discrepancy around 10 eV above the vacuum level is caused by the minimum in the InMFP of the electrons with those energies present here in our model.

The experimental results [17] show the well known

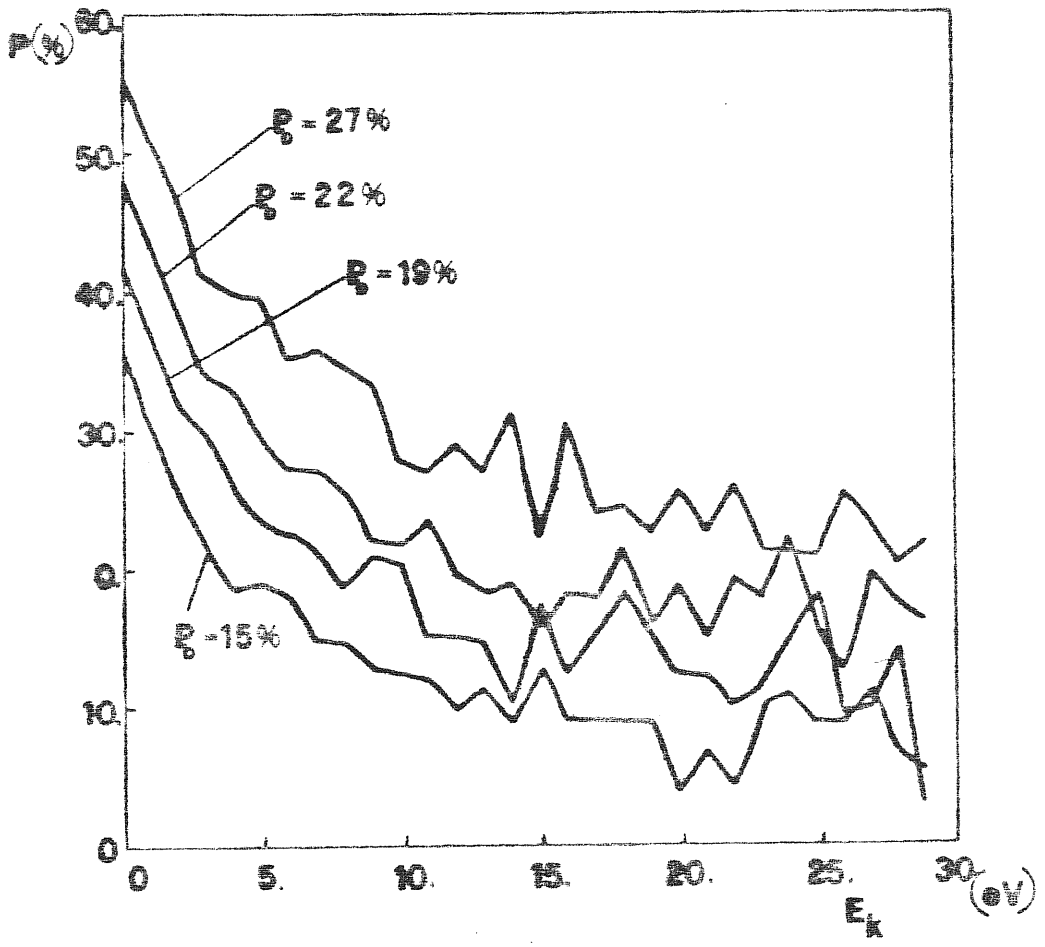

Fig.7

Polarization of SE obtained by computer simulation for different P_b values. The increase of ststistical noise with increasing kinetic energy E_k is caused by decreas of electron intensity (see Fig.8).

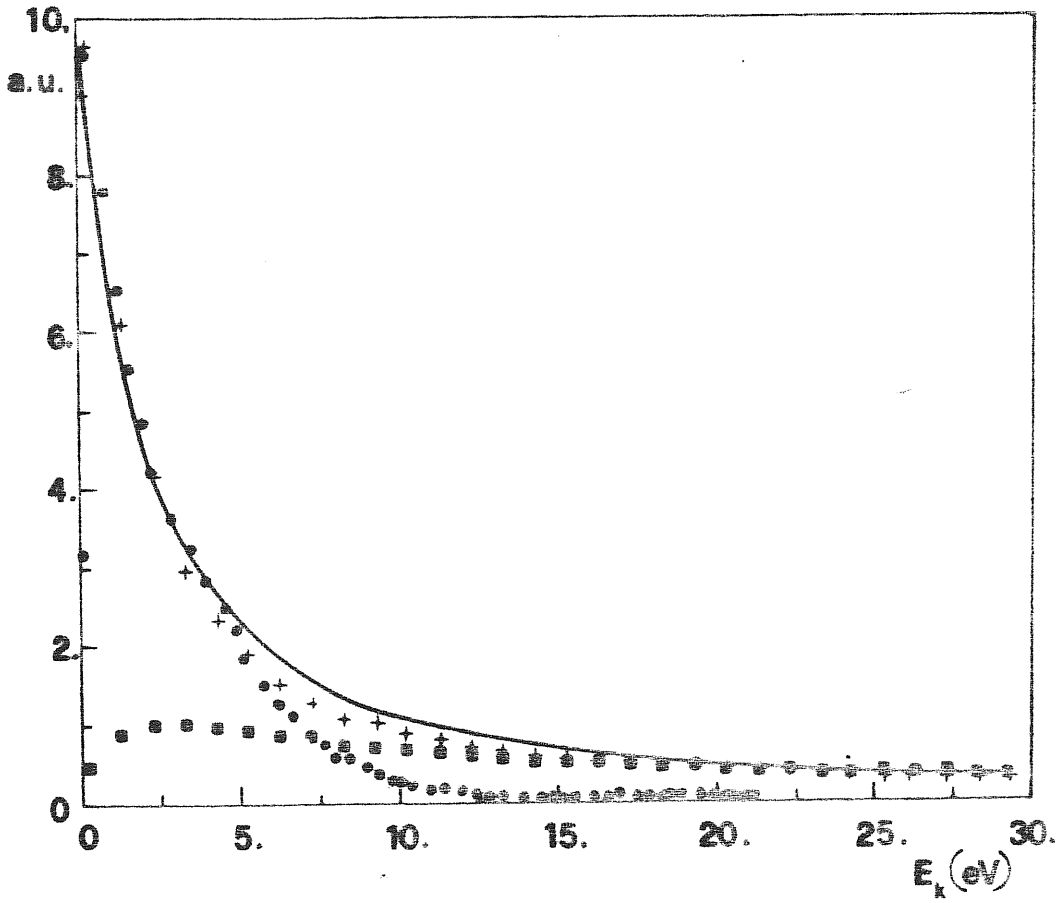

Fig.8

Energy distribution of secondary electron as a function of their kinetic energy; (•)-experiment; (+)-computer simulation; solid line - master equation solution. All intensities have been normalized to the value at E_k=0. (■)-intensity from the simulation with surface scattering. It has been matched at 15 eV with the intensity from computer simulation without surface scattering.

peak in the intensity of secondaries at almost zero kinetic enrergy--caused by the escaping mechanism. Of course, in the master equation solution as well as in the simulation without surface scattering the calculated maximum is instead at kinetic energy exactly zero. Except for that the agreement between experimental and theoretical results, especially for small energies is rather good. The excellent agreement of intensities predicted for small energies by the rate equation results with the experimental intensities is so good that it probably has some fortuitous element in it. It is very gratifying to find that the two independent methods, the computer simulation and the rate equation approach, agree so well.

For higher energies theoretical intensities are higher then experimental ones. This is because in the experiment a part of more energetic SE fail to be detected [17].

We also show in Fig.8 energy distribution of secondaries produced by the simulation with surface scattering, introduced by a potential step . As mentioned earlier the agreement with experiment is in this case not very good. If, as we believe, this is due to surface disorder, it would be interesting to check experimentally whether the lineshape of a crystalline ,ordered and flat surface has indeed this form.

In Fig.9 a,b & c we show spin polarization of secondaries for samples with different Fe/Ni composition. The agreement between experimental and theoretical ("theoretical" meaning computer simulation and master equation solution) results is in each case quite satisfactory.

The experimental "plateau" polarization around E_k = 15 eV is in general slightly larger than that obtained from the simulation. As is seen from Fig.7 the computer experiment is very sensitive to the parameter c of our

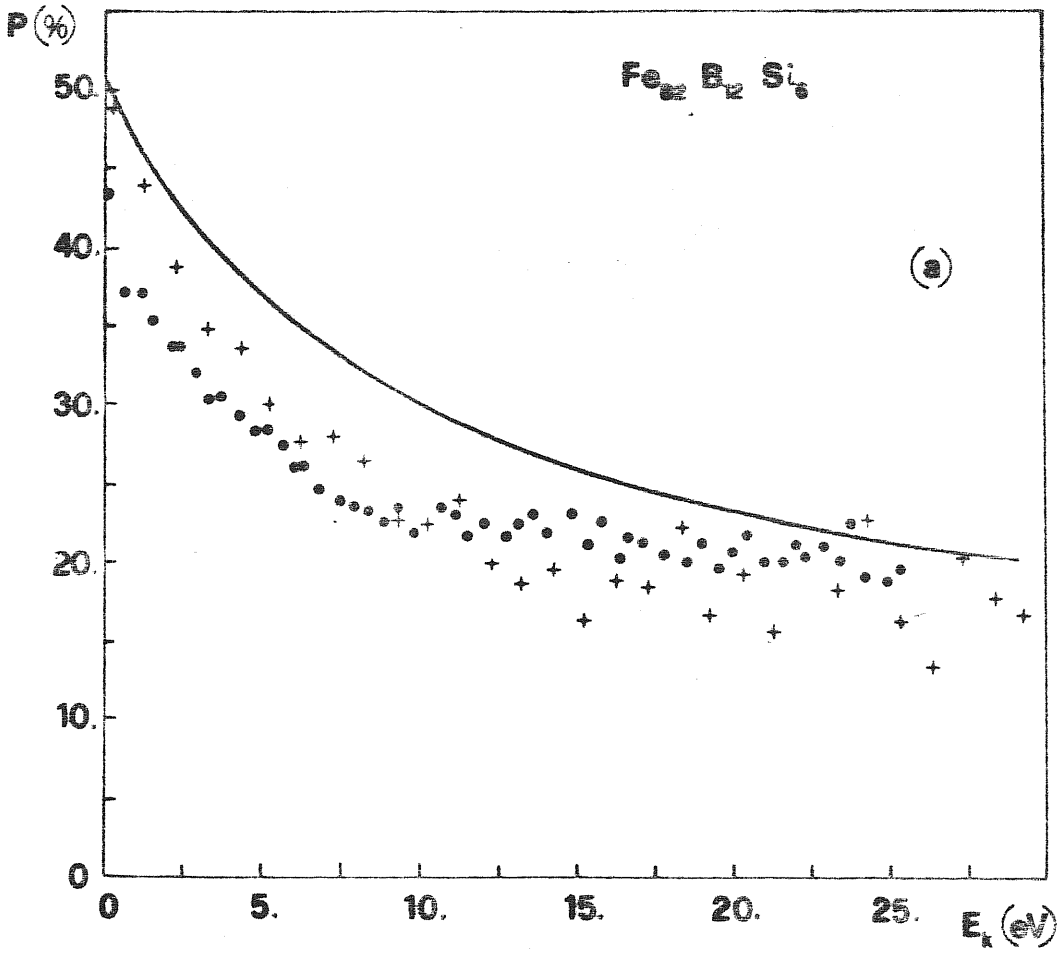

Fig.9 a)

Polarization of secondaries for P_b=22%; (•)-experiment, (+)-computer simulation, solid line - master equations solution. PE beam in experiment and simulation has the same parameters (also for Fig.9(b) and (c)): E_p=400 eV, =30°, unpolarized.

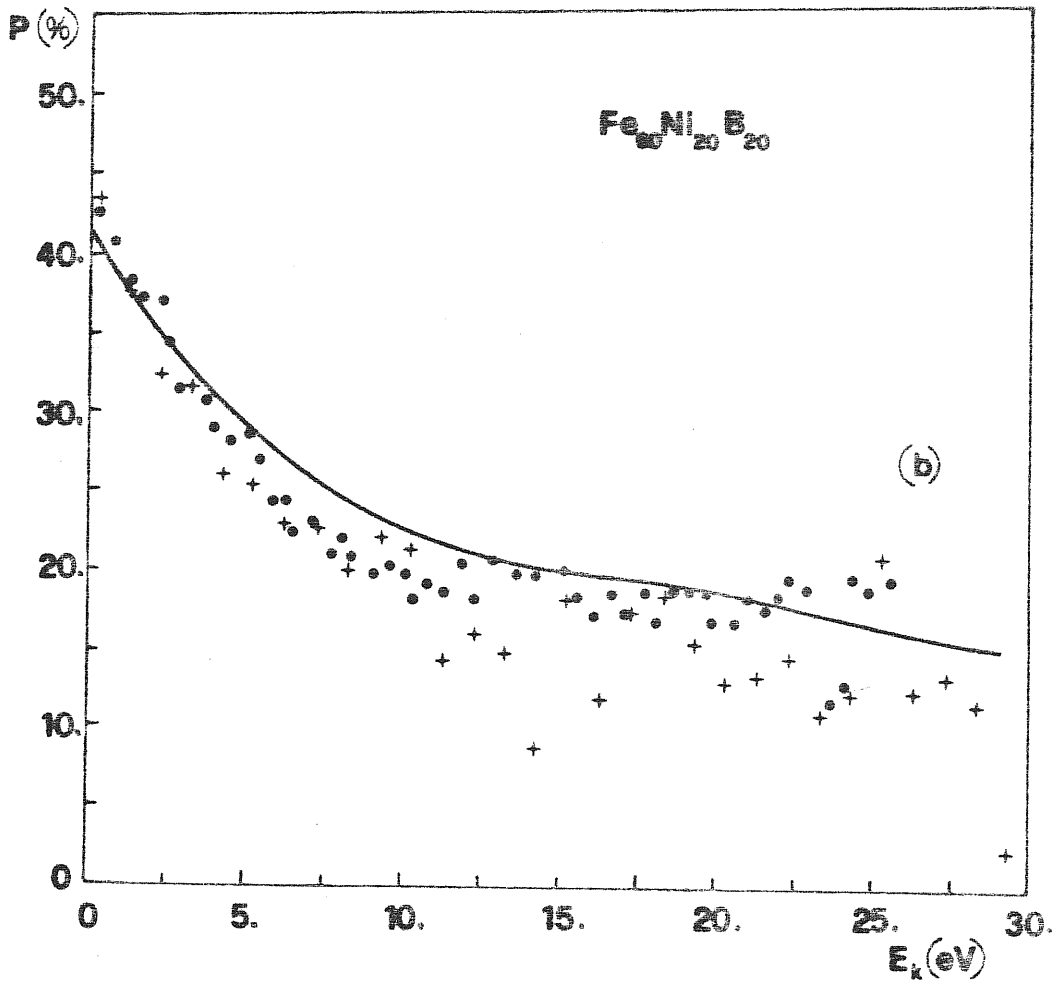

Fig.9 b)

Polarization of secondaries for P_b=19%; (•)-experiment, (+)-computer simulation, solid line - master equation solution.

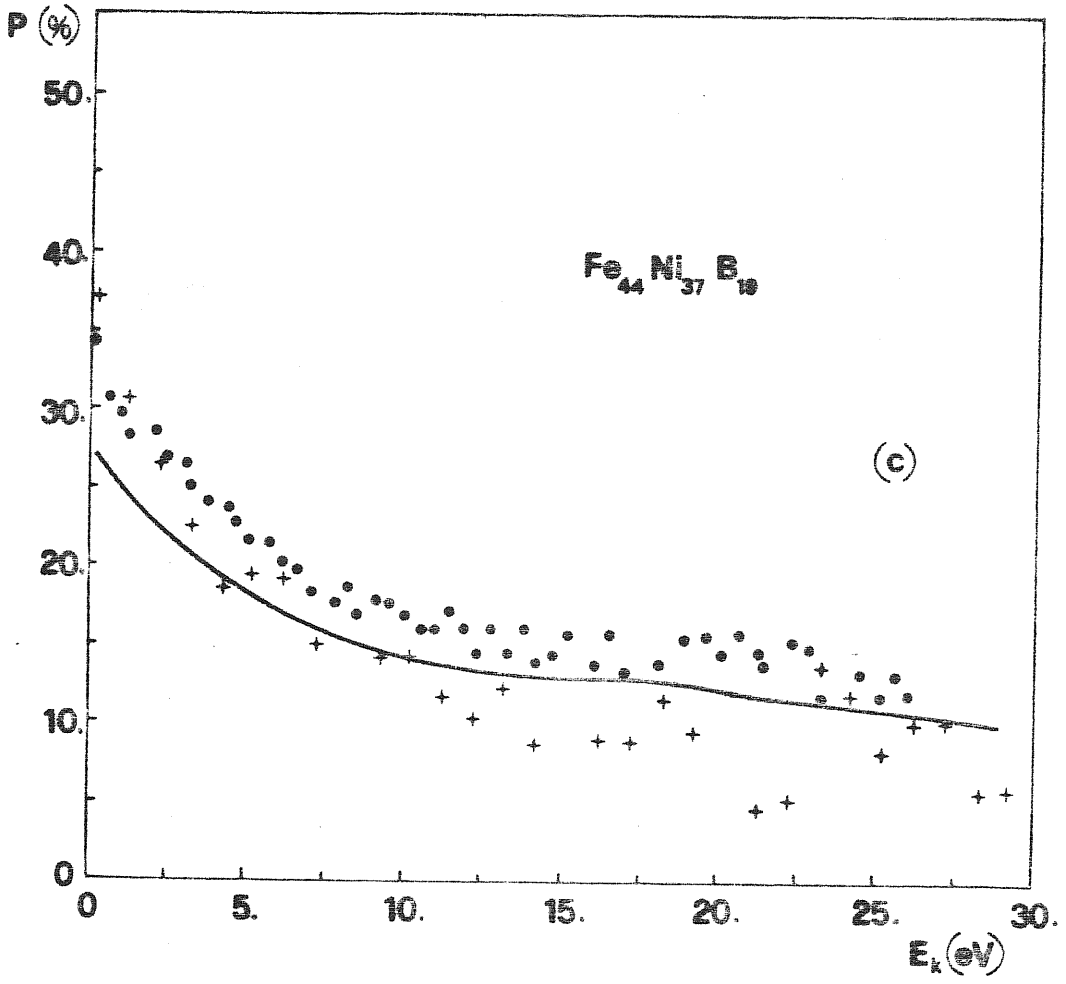

Fig.9 c)

Polarization of secondaries for P_b=15%; (•)-experiment, (+)-computer simulation, solid line - solution of master equations.

model. The small differences between real and computer experiment in the plateau region can in principle be adjusted by small changes in c .

There are two simultaneous mechanisms at work that determine the SE polarization at energies around 15 eV where the bulk plarization reached :
(i) the multiple scattering : this should enhance P to be larger than P_b , as seen for low E ,
(ii) suppression of exchange, for a high energy electron : interaction between electrons is in this case practically spin - independent and electrons excited randomly from conduction bands have to show up the bulk polarization P_b.
If the PE energy is small, say 50 eV or less, both mechanisms described above should be of smaller importance, and effects caused by the variation of surface magnetization with respect to the bulk one, can also be observed [34,38] (see also following subsection).

The experimental polarization decreases for increasing E_k, coming to a "plateau" from E_k=15eV onwards, where the polarization of secondaries is anyway close to the bulk polarization P_b. In the rate equation results P is also close to the P_b value but it keeps decreasing slowly with electron energy. The polarization obtained from rate equations are generally slightly larger than those from simulations. This is because of the assumption of the infinite solid inherent in our rate equation approach. In the simulation electrons can cross the surface before the polarization predicted by the rate equations is reached.

The simulation results are affected by a large statistical noise in the plateau region but they tend to in

dicate that when the low - energy secondary polarization is well reproduced in shape and magnitude, then a somewhat lower polarization than P_b is found in the high energy regime $E_k > 15$ eV. At present, it is not clear whether the origin of this slight disagreement is to be blamed on the experiment or the theory. In fact, while there are indications that in other cases polarization lower than P_b may be observed [34,38], we also have no guarantee that our theory is reliable at high energies where the collective excitations are also important.

We finally come to discuss the most interesting feature of the secondary polarization spectrum, namely the large polarization enhancement at small kinetic energy. This phenomenon has been so far somewhat puzzling. As Fig.9 a)b) and c) show, it is very well reproduced by our calculations. It thus establishes this enhancement as a bulk phenomenon, brought about by the multiple inelastic scattering.

The main and crucial reason for the existence of this enhancement can be simply stated as the fact that most spin - down electrons in the cascade, decay in energy with preferential and massive creation of Stoner excitations at $\omega \cong 2.2$ eV in Fe -based glasses. Electrons of down spin terminate their life by falling into the empty $d^{\downarrow}$ band, below the vacuum barrier. Since the same is not possible for up - spin electrons, this produces a "filtering" effect which reduces the down - spin secondary population. On top of this, as a result of the Stoner pair creation, an up spin electron emerges at energy $E - \omega$, which further enriches the up spin secondary population at low energy

side. Repeated occurence of the Stoner pair creation leads eventually to a very large increase of P at very low E_k.

In order to give further quantitative support for our statement, we have calculated the number of up - spin electrons between 0 and 1 eV kinetic energy which come from a Stoner pair excitation (i.e. the last inelastic event before leaving the metal was a Stoner excitation), and found them to be a large fraction , $\sim$ 38% of total number (for P_b = 27%).

The present calculations show good agreement between data taken in glasses with decreasing average magnetization and calculations done keeping the exchange splitting Δ constant and just changing the adjustable enhancement parameter c , which represents crudely the d - density of states near E_F . The results obtainable by keeping c constant and decreasing Δ would however not be very different.

3.3 Polarization of secondaries for ferromagnets with spatial variation of magnetization , primary energy dependence.

The computer simulation technique provides the possibility of a numerical study of the cascade process in a ferromagnet having magnetization varying in space. The original idea [21,34] is that changing the energy E_p of PE one changes their penetration depth. Hence, if magnetization is depth - dependent , one should observe primar energy dependence of SPSEE.

First, we check in our "computer experiment" how the density D(z) of hot electrons, created during the cascade process at a depth z below the surface, depends on primary energy E_p. We have found , running several simulations, D(z) for different E_p by counting the electrons with positive kinetic energy created at a depth z, after an inelastic scattering. The results are shown in Fig.10 . They are similar to those obtained also in the Monte-Carlo study by Gauchaud & Cailler [32]. However, in their study of spatial extent of the secondary process inside the metal, they were looking for the total energy loss as a function of the depth. This similarity between the two results is not unexpected, since the total energy loss and hot - electron density D are related through the average energy loss which we have actually found to vary slowly with z . For our purpose the density D is the more significant variable then the total energy loss.

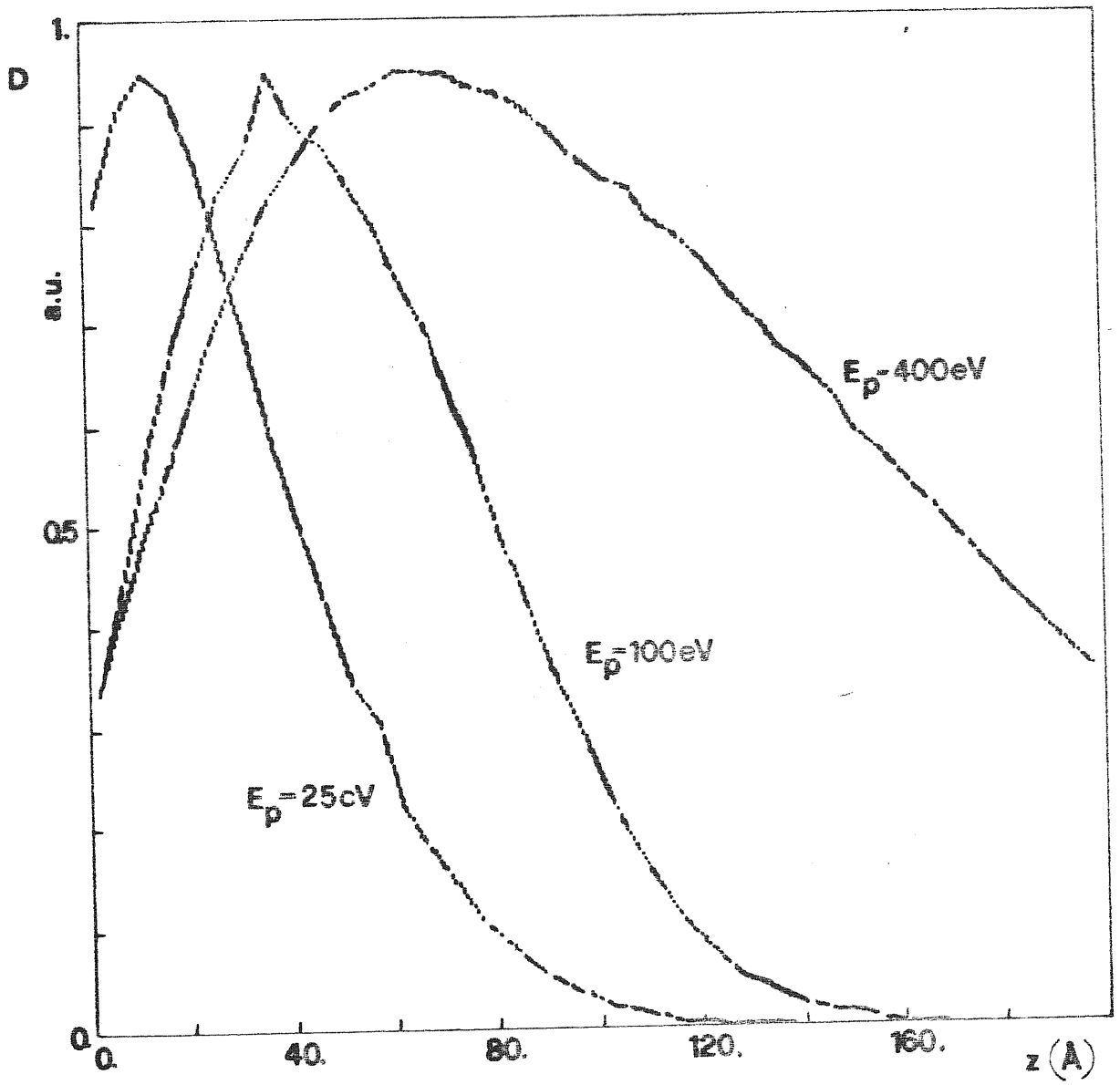

Fig.10

Density of hot electrons D as a function of the depth z below the metal surface, for different primary energies. The small wiggles are due to statistical noise. (Note that the "elastic mirror" depth which is six time the InMFP, see Fig.16, is much greater than the depth of the peak in D function, for each E_p respectively).

As it could be anticipated, with E_p increasing, the maximum of D shifts towards larger depths with electrons becoming more spread inside the metal. The depth resulting from our model should be suitably reduced when applied to real systems not with e - e scattering alone (see Ref.32 and discussion in Section 5.).

As pointed out in Ref.34 the chemical composition of metallic glasses can vary between the surface and the bulk. This can lead to a significant reduction of the magnetization towards the surface. However, the magnitude and spatial extent of that reduction is not known exactly. We are able to mimic such a situation within our simulation by continously changing the parameter c. We put $c = 0$ on the surface, which corresponds to $P_b = 10\%$ with the Stoner excitations almost completely suppressed, and increase it linearly with z up to the $c = 2$ ($P_b = 22\%$) for z approaching the limiting value z_b, which is thus the width of the transition region between the surface and the bulk. For $z > z_b$ c remains constant. We have run several simulations for different primary energies E_p and for three different z_b values : $z_b = 50$Å, $z_b = 35$Å and $z_b = 0$ ($z_b = 0$ means $c = 2$ for all z). We have looked for polarization in the plateau region P_{pl} defined as the average polarization of electrons emitted with kinetic energies in the energy range between 13 and 17 eV (see Fig.11). As expected for $z_b = 50$Å & $z_b = 35$Å, the polarization P_{pl} increasies with increasing primary energy E_p. The reason is that for more energetic primaries, electrons penetrate deeper into the solid (see Fig.10) where the bulk polarization is larger than close to the surface. For high

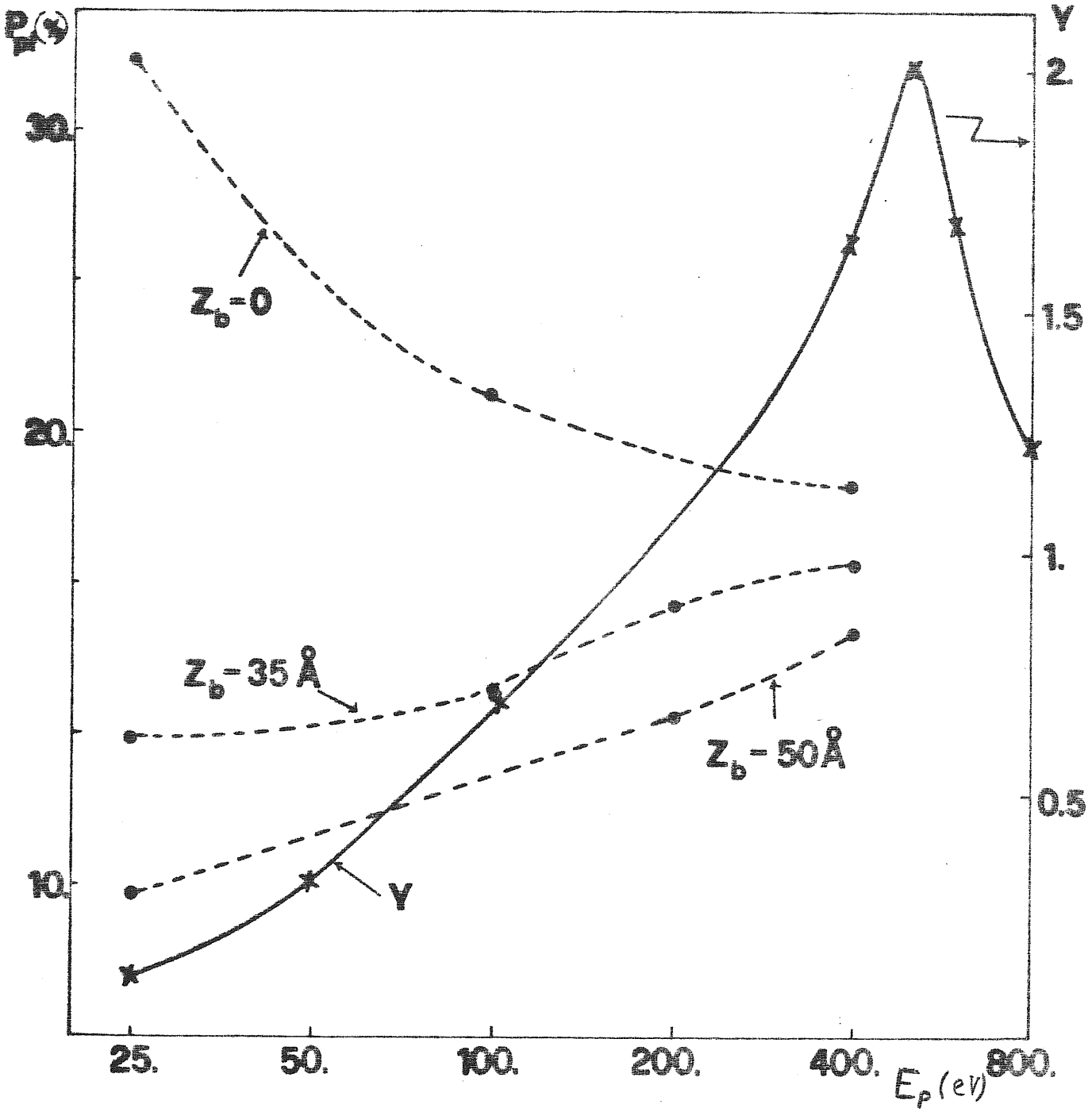

Fig.11

Average polarization for secondaries with kinetic energies between 13 eV and 17eV as a function of primary energy E_p for different magnetization profiles, and the total yield Y of secondaries as the function of E_p. The statistical errors in polarization are less than 2% [i.e. $P_{pl} \rightarrow (P_{pl} \pm 2\%)$]

enough primary energies, when the mean - free - path of primary electron is much bigger then z_b, saturation has to be reached, which has actually been experimentally observed by Mauri [34] in $Fe_{83}B_{17}$ ferromagnetic glass for E_p = 300 eV. In our "computer experiment" the saturation is almost reached for E_p = 400 eV, at least for z_b = 35Å (which for technical reasons is the highest primary energy we can fully study). The escape mechanism obviously prefers electrons close to the surface to leave the solid, so the saturation value of P_{pl} should lie somewhere between those surface and deep ($z > z_b$) bulk polarization.

The results for z_b=0 (no surface reduction of the magnetization), shown in Fig.11, require a separate explanation. At first sight it seems surprising that the plateau polarization P_{pl} is the largest for the smallest primary energy, E_p = 25 eV, and is much larger than the bulk polarization. It is not so surprising, however, if one considers that the primaries with E_p = 25 eV fall down to the energy region between 13 eV and 17 eV after only one or two inelastic events. For those primary energies, exchange Stoner excitations are strongly enhanced which leads to the large polarization of scattered electrons (see Fig.5). Actually we show here that the measurements of the outgoing electron polarization averaged over a relatively wide energy range can be used as an alternative method for the observation of Stoner excitations in the strong ferromagnets. The main advantage of this method is that it does not require high enery resolution in the detection of secondaries. With increasing primary energy E_p

the cascade develops fully, as discussed in detail in Section 3.2. As a result, for primary energies E_p, above 200eV low energy electrons emitted from the solid practically do not carry any information about primaries and P_{pl} remains almost flat (see Fig.11 ; $z_b = 0$).

We show, also in Fig.11, the total yield of secondaries Y. The primary energy dependence of Y we obtained resembles that observed by Mauri [34], especially for primary energies below 400eV. We have also found a maximum in the total electron yield Y, resulting from a competition between secondary production and penetration of primaries. Both of them increase with increasing E_p, around the same energy as Mauri did, namely E_p=500eV. Our maximum is however much sharper. The reason for this is undoubtedly the artificial way in which the elastic scattering in our simulation has been introduced (see previous subsection). Ganachaud & Cailler [32] have shown that the elastic mean-free-path grows slower then the inelastic one with E_p increasing, reducing thus the rate the penetration depth increases with, for increasing primary energy. This leads to the flatter aspect of the maximum in the total yield Y, that they found in their simulation [32].

4. PARAMAGNETIC METALS.

The well-established technique based on GaAs polarized electron guns and Mott scattering spin analyzers , makes in principle possible an experiment with spin - oriented electron PE beam and spin - analyzed scattered electrons . This type of measurement gives a new opportunity of direct observation of exchange process between primary and paramagnetic - metal electrons [39] . In this Section we present our theoretical prediction for such an experiment. We give a quantitative description of the exchange process in terms of depolarization of initially fully polarized PE beam using a model of a paramagnetic metal consisting of a single parabolic band filled up to the Fermi level E_F . Within this free electron approximation of a real paramagnet, which seems quite reasonable for a simple metal, such as Al, we calculate the single scattering rates in the first order perturbation theory for direct and exchange process. A comparison with Møller [6,7] scattering of two electrons is also presented. In Møller scattering the exchange process becomes negligible with respect to the direct scattering when the energy loss goes to zero. We show in detail that this is no longer the case for electrons scattered by a Fermi sea. Our results indicate that the exchange spin - flip process should be generally easy to observe and should reveal a relation between the relative flip probability and the metal screening properties.

The single scattering theory can be applied direc-

tly only to electrons which leave the metal with energy loss of the order of a few electronvolts. In fact, for an energetic PE , a small energy loss has a low probability, which makes multiple inelastic scattering practically negligible. We have also calculated the polarization of scattered electrons with energies very much smaller than E_p , namely secondaries, solving as in Section 3.1 the equilibrium rate equations. The results indicate the possobility for observing a weak exchange-induced spin-down polarization of secondaries, for a spin up primary(*).

(*) We concentrate here only on spin-effects caused by inelastic scattering. The spin-orbit polarization effects present in electron-ion scattering can be eliminated by: proper experimental conditions, such as (i) use of PE with polarization parallel to the electron beam; and/or (ii) use of PE with alternate polarization, and then : average between the data thus obtained.

4.1 Inelastic scattering rates.

The model of a paramagnetic metal which we will use here is a special case of the model introduced in Section 2, with $c=\Delta'=0$. We repeat, however, the main steps in the procedure of calculating spin-resolved inelastic rates, for the purpose of further discussion. The technique of calculation used here is fully reported in Ref.18.

The spin-flip scattering rate $R^{\uparrow\downarrow}(E,\omega)$ of the electron from the state $E,\vec{p}$ to the final state $E-\omega$, $(\vec{p}-\vec{q})$, with momentum transfer $\vec{q}$ and energy transfer ω between antiparallel spin electrons, is proportional in lowest order perturbation theory to the imaginary part of scattering amplitude :

$$R^{\uparrow\downarrow}(E,\omega) = -\frac{2}{\pi}\,\mathrm{Im}\int\!\!\int d\xi^{7}\,|V(\vec{p}-\vec{q}-\vec{k})|^{2}\times$$
$$\times G^{e}(E-\omega,(\vec{p}-\vec{q})^{\downarrow})\times$$
$$\times G^{e}(\epsilon+\omega,(\vec{q}+\vec{k})^{\uparrow})\times \qquad (24)$$
$$\times G^{h}(\epsilon,\vec{k}^{\downarrow})\Big]\,,$$

where

$$d\vec{\zeta}^{\,7} = \frac{d^3q}{(2\pi)^3} \cdot \frac{d^3k}{(2\pi)^3} \cdot \frac{d\epsilon}{2\pi} \quad ,$$

and the electron (hole) Green's function is given by :

$$G^{e(h)}(\epsilon, \vec{k}) = \frac{1}{\epsilon - \epsilon_{\vec{k}} \pm i0^+} \quad , \tag{25}$$

with

$$\epsilon_{\vec{k}} = \frac{k^2}{2m} \quad . \tag{26}$$

The non-flip scattering rate $R^{\uparrow\uparrow}(E, \omega)$ is given as the sum of four terms :

$$R^{\uparrow\uparrow}(E,\omega) = R_1^{\uparrow\uparrow}(E,\omega) + R_2^{\uparrow\uparrow}(E,\omega) + R_3^{\uparrow\uparrow}(E,\omega) + 2R_4(E,\omega), \tag{27}$$

where

$$R_1^{\uparrow\uparrow}(E,\omega) = -\frac{2}{\pi} \mathrm{Im}\left[\int d\vec{\zeta}^{\,7} |V(\vec{q})|^2 G^e(E-\omega, (\vec{p}-\vec{q})^\uparrow) \times \right. \tag{28a}$$

$$\left. \times G^e(\epsilon+\omega, (\vec{q}+\vec{k})^\uparrow) G^h(\epsilon, \vec{k}^\uparrow)\right] ,$$

$$R_2^{\uparrow\uparrow}(E,\omega) = -\frac{2}{\pi}\,\mathrm{Im}\Big[\int d\vec{q}\,|V(\vec{q})|^2 G^e(E-\omega,(\vec{p}-\vec{q})^{\uparrow}) \times$$

$$\times\, G^e(E+\omega,(\vec{q}+\vec{k})^{\downarrow})\, G^h(E,k^{\downarrow})\,, \qquad (28b)$$

$$R_3^{\uparrow\uparrow}(E,\omega) = -\frac{2}{\pi}\,\mathrm{Im}\Big[\int d\vec{q}\,V(\vec{p}-\vec{q},-\vec{k})^2 \times G^e(E-\omega,(\vec{p}-\vec{q})^{\uparrow}) \times$$

$$\times\, G^e(E+\omega,(\vec{q}+\vec{k})^{\uparrow}\, G^h(E,k^{\uparrow})\,, \qquad (28c)$$

and

$$R_4^{\uparrow\uparrow}(E,\omega) = -\frac{2}{\pi}\,\mathrm{Im}\Big[\int d\vec{q}\,V(\vec{q})V(\vec{p}-\vec{q},-\vec{k}) \times \qquad (28d)$$

$$\times\, G^e(E-\omega,(\vec{p}-\vec{q})^{\uparrow})\, G^e(E+\omega,(\vec{q}+\vec{k})^{\uparrow}) \times$$

$$\times\, G^h(E,\vec{k}^{\uparrow})\,.$$

For clarity we have put spin indexes into the formulas; however, the Green's functions do not depend on them here. The first two terms $R_1^{\uparrow\uparrow}$, $R_2^{\uparrow\uparrow}$ represent direct process where the incoming up-spin electron is scattered against another up and down spin electron respectively. Since, there is an equal number of up and down-spins in the paramagnet, $R_1^{\uparrow\uparrow}(E,\omega) = R_2(E,\omega)$. The third partial term $R_3(E,\omega)$ represents the exchange

non-flip process. Again, since $n^{\uparrow} = n^{\downarrow}$, this rate is numerically equal to the rate of exchange spin-flip process, $R_3^{\uparrow\uparrow}(E,\omega) = R^{\uparrow\downarrow}(E,\omega)$. This does not mean that spin-flip and non-flip exchange processes have equal probabilities. The probability of exchange process between parallel-oriented spins is diminished by the negative term $2R_4$ which represents the quantum-mechanical interference between direct and exchange amplitudes. (In fact, this is the point where indistinguishability of particles comes in).

The values of $R^{\downarrow\uparrow}(E,\omega)$ and $R^{\downarrow\downarrow}(E,\omega)$, for incoming down-spin electrons, are the same as for incoming up-spin electrons.

As an interaction between electrons we use again the statically screened Coulomb potential as in Eq.6. The many-body effects, e.g. plasmon scattering, are not present in this model. However, they should not be important for very small energy losses ($\omega < \omega_p$).

With this electron-electron interaction we can perform the five out of seven integrations in Eq.24-28 analytically, while two are left for numerical calculations. We have used E_F = 11.7 eV and a work function ϕ =4.25 eV, a choice of parameters appropriate for Al.

Having obtained $R^{\uparrow\uparrow}$ and $R^{\uparrow\downarrow}$, we can find the final polarization $P_{out}(E,\omega)$ of initially spin-up polarized electron after a single inelastic event :

$$P_{out}(E,\omega) = \frac{R^{\uparrow\uparrow}(E,\omega) - R^{\uparrow\downarrow}(E,\omega)}{R^{\uparrow\uparrow}(E,\omega) + R^{\uparrow\downarrow}(E,\omega)} \quad . \quad . \qquad (29)$$

The polarization P_{out} is not labeled any spin index, since its value is the same for either up and down incoming spins.

In Fig.12 we show the single scqttering energy loss rates $R^{\uparrow\uparrow}$ and $R^{\uparrow\downarrow}$ for a fixed primary enrgy (kinetic) E_p = 120 eV, as a function of the final kinetic energy E_k, defined by Eq.4. In terms of the energy loss ω, E_k is given by :

$$E_K = E_p - \omega \quad . \qquad (30)$$

For E_k approaching E_p, the scattering rate $R^{\uparrow\uparrow}$ goes to zero, as evident from phase space considerations, since the number of conduction electrons which can be excited above E_F also goes to zero. Similarly, around $E_p - E_k = E_F$; all the conduction electrons begin to have a chance to be excited (predominantly during direct scattering) whence the maximum of $R^{\uparrow\uparrow}$;(see Eq. 28 a) and b)).

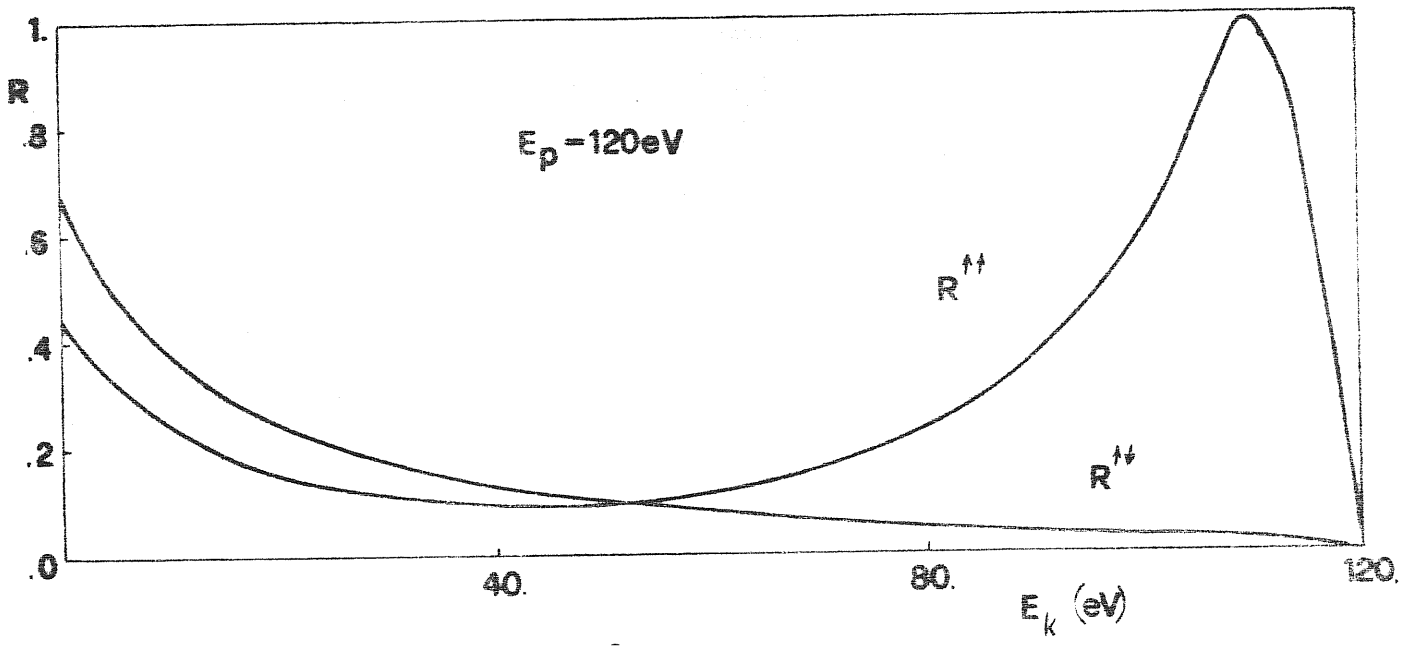

Fig.12

Flip $R^{\uparrow\downarrow}$ and non-flip $R^{\uparrow\uparrow}$ inelastic scattering rates as the function of kinetic energy of scattered electron.

The increase of $R^{\uparrow\uparrow}$ for small E_k is caused by the increase of the exchange term $R_3^{\uparrow\uparrow}$ (Eq.28 c). (In some sense this is a replica of the maximum around $\omega = E_F$).
In our calculations we fix the energy of an observed electron and integrate over all other variables, in particular on the momentum of the second electron (equal to $\vec{q}+\vec{k}$ in our formalism).

The rate $R^{\uparrow\downarrow}$ is a pure exchange processes. For small energy losses $R^{\uparrow\downarrow}$ is much smaller than $R^{\uparrow\uparrow}$, since in those cases exchange scattering requires a large momentum transfer which implies, by Eq.6, a small $|V|^2$. With increasing energy loss, the exchange process eventually overcomes the non-flip process, at about $E_p/2$. This is because of the negative interference term $2R_4^{\uparrow\uparrow}$, which diminishes non-flip rates (otherwise, for small E_k, with $R_1^{\uparrow\uparrow}$ and $R_2^{\uparrow\uparrow}$ becoming negligible, $R^{\uparrow\downarrow}$ and $R^{\uparrow\uparrow}$ would be equal).

In Fig.13 we show P_{out} defined by Eq.29, compared with that calculated in the non-relativistic limit for two-electron scattering (Møller scattering).
The shape of the two curves in Fig.13 is very similar.
It indicates, that for a rough estimate of the importance

of the exchange interaction of an energetic electron with a paramagnetic metal, one can use just the scattering theory of two free electrons. However, there is an important difference of detail, which we describe next.

4.2 Depolarization for small energy losses.

In this section we discuss the differences between spin-flip Møller scattering, and that from a paramagnetic metal, when the energy loss is small.

For small ω (E_k approaching E_p) the polarization of an electron scattered off another single electron at rest remains 100% (see Fig.13), for all primary energies E_p. Physically this means that in that reference system the exchange process rate goes to zero much faster than the rate for the direct process.

In the other case of electron-paramagnet scattering, on the other hand, a finite depolarization is found for $\omega \to 0$ (see Fig.13). In fact, in this case the electron is scattered on those Fermi sea electrons which have momenta of the order of Fermi momentum $p_F = (2mE_F)^{1/2}$. This makes processes with infinitesimal energy loss and finite momentum transfer possible. Obviously, with $\omega \to 0$, the exchange scattering rate does again go to zero (see Fig.12), but in a weaker way than for Møller scattering. The effect should be enhanced when primary momentum p becomes comparable with p_F. To be more precise, let us define $P_o(E_p)$ as the limit of $P_{out}(E_p, \omega)$ for $\omega = 0$:

$$P_o(E_p) = \lim_{\omega \to 0} \frac{R^{\uparrow\uparrow}(E_p,\omega) - R^{\uparrow\downarrow}(E_p,\omega)}{R^{\uparrow\uparrow}(E_p,\omega) + R^{\uparrow\downarrow}(E_p,\omega)} \quad . \tag{31}$$

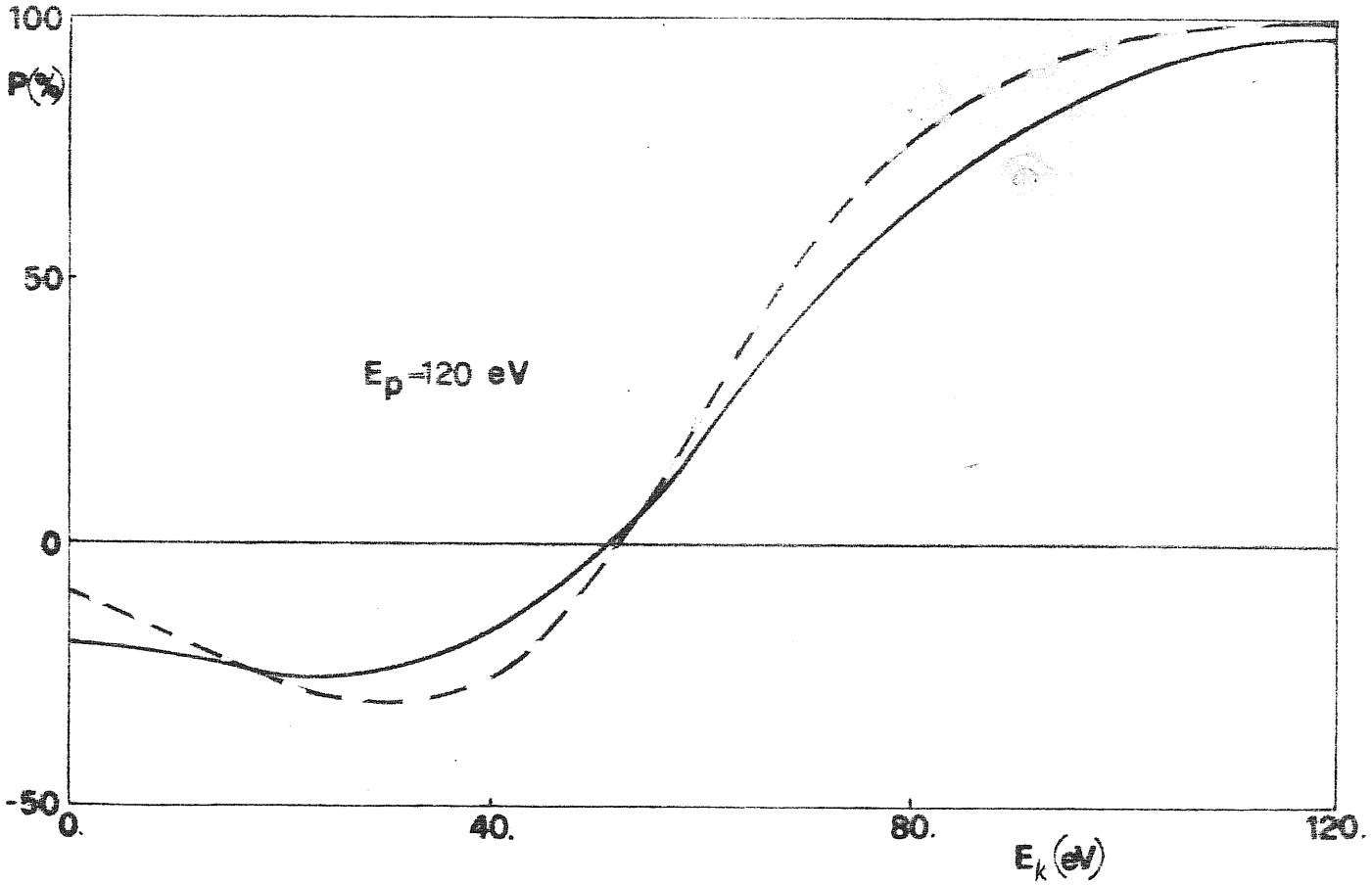

Fig.13

Polarization of scattered electron versus final kinetic energy. Solid line - present model. Dashed line - Møller scattering of two free electrons.

Using Eq. 24-28,31 we have calculated P_o for ω approaching zero. The result is shown in Fig. 14. For large E_p, $R^{\uparrow\uparrow} >> R^{\uparrow\downarrow}$, we can rewrite therefore Eq.31 in the simpler form :

$$P_o(E_p) \simeq \lim_{\omega \to 0} 1 - 2 \frac{R^{\uparrow\downarrow}(E_p, \omega)}{R^{\uparrow\uparrow}(E_p, \omega)} \quad . \tag{32}$$

For infinitesimal energy loss the momentum transfer wave vector q is limited by Fermi surface : $0 \lesssim q \lesssim 2p_F$. Thus, if the primary momentum $p = (2m(E_p + V_o))^{1/2}$ is much greater than q_{FT}, the non - flip scattering rate $R^{\uparrow\uparrow}$ has its main contributions from the partial scattering rates $R_1^{\uparrow\uparrow}$ and $R_2^{\uparrow\uparrow}$ (see Eq.6,24-28). Neglecting q_{FT}, q and k (k is always smaller than p_F) and leaving only the primary momentum p in the matrix element in the formula for flip rate $R^{\uparrow\downarrow}$ (Eq.24) we can write :

$$R^{\uparrow\downarrow}(E_p, \omega)\Big|_{\substack{E_p \to \infty \\ \omega \to 0}} = \frac{\alpha}{P} \int_0^{2p_F} dq \int_{\sqrt{2m(E_F-\omega)}}^{p_F} dk \cdot k \cdot \frac{1}{p^4} \quad , \tag{33}$$

and for non - flip rate :

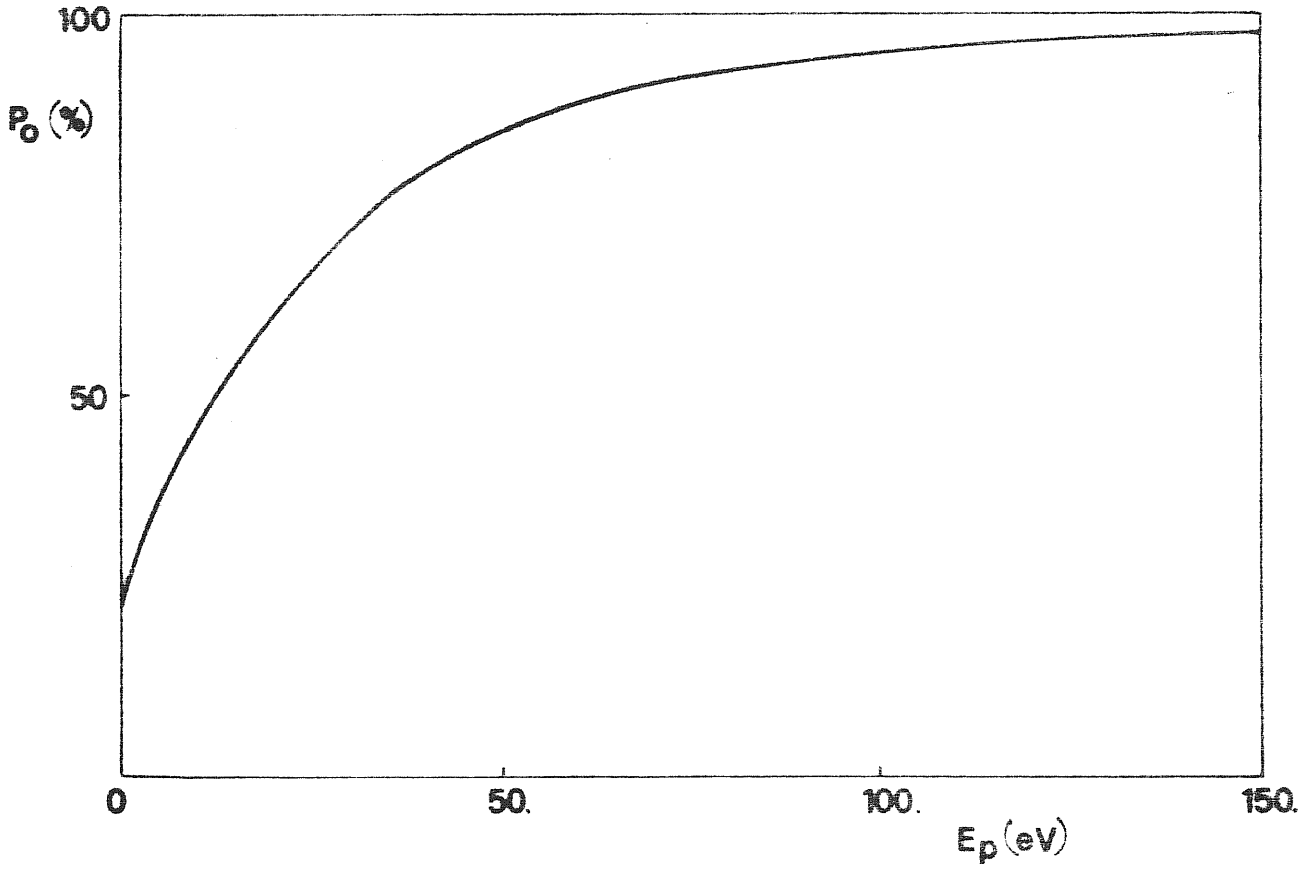

Fig.14

Depolarization of fully polarized primary electron beam by an infinitesimal energy loss as a function of primary energy.

$$R^{\uparrow\uparrow}(E_p,\omega)\Big|_{\substack{E_p\to\infty\\ \omega\to 0}} = \frac{\alpha}{p}\,2\int_0^{2p_F} dq_\perp \int_{\sqrt{2m(E_F-\omega)}}^{p_F} dk\cdot k\cdot \frac{1}{(q^2+q_{FT}^2)^2}\,, \qquad (34)$$

where α is a constant.

Putting Eq. 33 & 34 into Eq.32 one easily obtains :

$$P_0(E_p) = 1 - \frac{2p_F / p^4}{\frac{1}{2q_{FT}^3}\,\mathrm{arctg}\left(\frac{2p_F}{q_{FT}}\right) + \frac{p_F}{q_{FT}^2\,(4p_F^2+q_{FT}^2)}}\,. \qquad (35)$$

Eq.35 is strictly valid for large primary energies E_p. By comparing this approximate P_o with accurate numerical results of Fig.14, we find that at least for the case of Al Eq.35 turns to be quite accurate for $E_p > 50$eV.

It is interesting to discuss the two special limits $q_{FT} \to 0$ and $p_F \to 0$ (note however that usually q_{FT} and p_F are fixed: $q_{FT}/p_F = 1.18$ for Al).

a). $q_{FT} \to 0$, p_F - finite

$$P_0(E_p) = 1 - \frac{8}{\pi} \cdot \frac{p_F q_{FT}^3}{p^4} \quad . \tag{36}$$

This formula represents the true results with good accuracy for $q_{FT} \ll p_F$.
It shows directly that a finite depolarization of electron scattered inelastically on the metal electrons with small energy loss is caused both by existence of a Fermi surface as well as by free-electron screening.

b). q_{FT} - finite , $p_F \to 0$

$$P_0(E_p) = 1 - \frac{q_{FT}^4}{p^4} \quad . \tag{37}$$

This limit is extremely interesting from the theoretical point of view : $p_F \to 0$ means that Eq. 37 describes the Møller scattering of two electrons interacting by a screened Coulomb potential, treated in the Born approximation.
The fact that screening enhances the exchange amplitude with respect to the direct one has already been pointed out by Matthew [40]. For small energy losses the direct scattering rate is governed by momentum transfer q (see Eq. 34). The introduction of q_{FT}, comparable with q, reduces the probability of direct process, while the

exchange one, governed by the primary momentum p, remains almost unaffected. The depolarizing effect of small energy loss single inelastic scattering from a paramagnetic metal shown on Fig.13 & 14 should be easily detectable experimentally.

4.3 The secondary cascade - rate equation approach.

We have discussed up to now the single scattering energy loss. Fig.13 shows that an initially up-polarized electron preferentially reverses its polarization after losing most of its energy in a single scattering event. This reversed or negative polarization is as large as 30% for Al. Initially this number provides a direct measurement of the relative importance of the Pauli principle at E_p=120eV: an up-spin electron still has 30% larger preference to scatter off a down spin electron below E_F, than one with same spin. In this energy region, however, the spectrum of emitted electrons is dominated by secondaries, which have been inelastically scattered many times in a cascade process. Since the cascade develops in a magnetically neutral medium, one can expect that the effect of the negative polarization should be diminished.

To obtain a quantitative answer to that problem we use again the rate equilibrium equations, already introduced in Section 3 :

$$\int_0^{E_p+V_0-E} d\omega \left[I^{\uparrow}(E+\omega) R^{\uparrow\uparrow}(E+\omega,\omega) + I^{\downarrow}(E+\omega) R^{\downarrow\uparrow}(E+\omega,\omega) \right] =$$

$$= I^{\uparrow}(E) \int_0^{E-E_F} d\omega \left[R^{\uparrow\uparrow}(E,\omega) + R^{\downarrow\uparrow}(E,\omega) \right] , \qquad (38a)$$

$$\int_0^{E_p+V_o-E} d\omega \left[I^{\downarrow}(E+\omega)\, R^{\downarrow\downarrow}(E+\omega,\omega) + I^{\uparrow}(E+\omega)\, R^{\uparrow\downarrow}(E+\omega,\omega) \right] =$$

$$= I^{\downarrow}(E) \int_0^{E-E_F} d\omega \left[R^{\downarrow\downarrow}(E,\omega) + R^{\downarrow\uparrow}(E,\omega) \right]. \qquad (38b)$$

Where the functions $I^{\uparrow}(E)$ and $I^{\downarrow}(E)$ are unknown. We have solved Eq.38 a) & b) numerically by the iteration procedure (described in Section 3.1) with the boundary condition of 100% - polarized PE (i.e. $I^{\uparrow}(E_p + V_o) = 1$, $I^{\downarrow}(E_p + V_o) = 0$) and for $V_o < E < E_p + V_o$. Having so obtained $I^{\uparrow}(E)$, $I^{\downarrow}(E)$, we can find (Eq.16 & 17) the intensity I(E) and polarization P(E) of hot electrons. The question arises, if I(E) and P(E) are closed to what we expect to be obsertved outside the metal ?

We show our resulting P(E) and P(E) on Fig.15, as was expected, the maximum negative polarization is reduced for E_p = 120 eV, by about a factor two with respect to the single scattering predictions (see Fig. 13), and

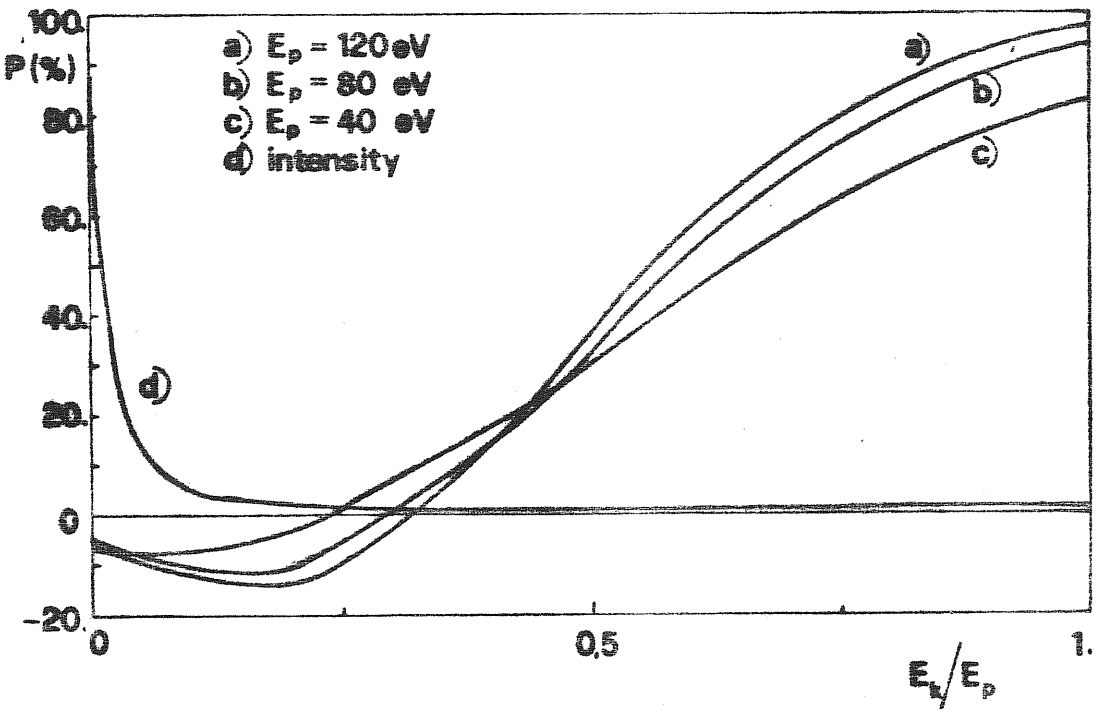

Fig.15

Polarization of secondaries emitted from Al for polarized primaries a)b)c) for different primary energies, and intensity in arbitrary units d) for E_p=120eV, versus reduced kinetic energy.

by about a factor four for small kinetic energies, but it is still of considerable magnitude. It should be quite easily detectable in an experiment, especially because of the high intensity of electrons emitted in that energy range. With increasing energy of emitted electrons the polarization should be more and more as predicted by single scattering theory. Actually, for large E_p only the very low energy part of this curve would be modified by the secondary cascade. This is the reason for the increased negative polarization with increasing E_p seen on Fig. 15.

For small energy losses, the results given by the master equation are very close to those given by single scattering. In particular, they give exactly the same finite depolarization for $\omega \to 0$, since then no cascade can ensue.

5. SPIN - DEPENDENCE OF INELASTIC MEAN-FREE-PATH OF ELECTRONS IN FERROMAGNETS.

It is reasonable to expect the inelastic men-free-path of an electron, in a material with different electronic structure for majority (up) and minority (down) spin orientation, to be dependent on its spin direction [41,42]. The early idea of Erskine & Stern [41] was that minority-spin electron, in Ni should have a smaller In^{MFP} than majority ones, since near to the Fermi level the density of states of minority spins is much greater than that of majority spins, thus causingng spin-down electrons to decay preferentially. Bringer et al. [9] and Feder [43] argued that exchange interaction should strongly prefer scattering between antiparallel-spin electrons, and gave a rough estimation for ratio between up and down In^{MFP} :

$\lambda^{\uparrow}/\lambda^{\downarrow} \sim n^{\uparrow}/n^{\downarrow}$.

The subsequent calculations of Rendell & Penn [44] yielded a considerable spin-asymmetry for (Ni,Co,Fe) A of the InMFP defined as :

$$A(E) = \frac{\lambda^{\uparrow}(E) - \lambda^{\downarrow}(E)}{\lambda^{\uparrow}(E) + \lambda^{\downarrow}(E)} , \qquad (39)$$

However, these authors predict a negative sign of A in contradiction to

Ref. 9,41,43) for Co and Fe and for small energies - - $E < 50$ eV).

These results have been criticized by Matthew [40], who also found a spin - dependence of InMFP much smaller than the predictions of Bringer et al. [9]. His "atomic" approximation however is valid only for primary energies $E_p > 100$ eV.

In this Section we calculate electron - electron part of InMFP $\lambda_{ee}^{\uparrow(\downarrow)}$. We use here the model introduced in Section 2, where the Coulomb potential with Thomas-Fermi screening is used as the e-e interaction.

Having the loss probabilities per unit time and per unit energy range of up and down spins calculated in Section 2 we can write the mean free path as

$$\lambda_{ee}^{\uparrow(\downarrow)}(E) = v^{\uparrow(\downarrow)}(E) \Big/ \int_0^{E-E_F} d\omega \left(R^{\uparrow(\downarrow)\uparrow}(E,\omega) + R^{\uparrow(\downarrow)\downarrow}(E,\omega) \right), \qquad (40)$$

where $v^{\uparrow(\downarrow)}(E)$ is the velocity of up (down) electron defined in Section 3.2.

We show on Fig.16 results for different bulk plarization $P_b = 27\%$ ($c = 3$ in this case) is the bulk polarization of crystalline ferromagnetic iron. The smaller P_b values correspond to less polarized iron based glasses.

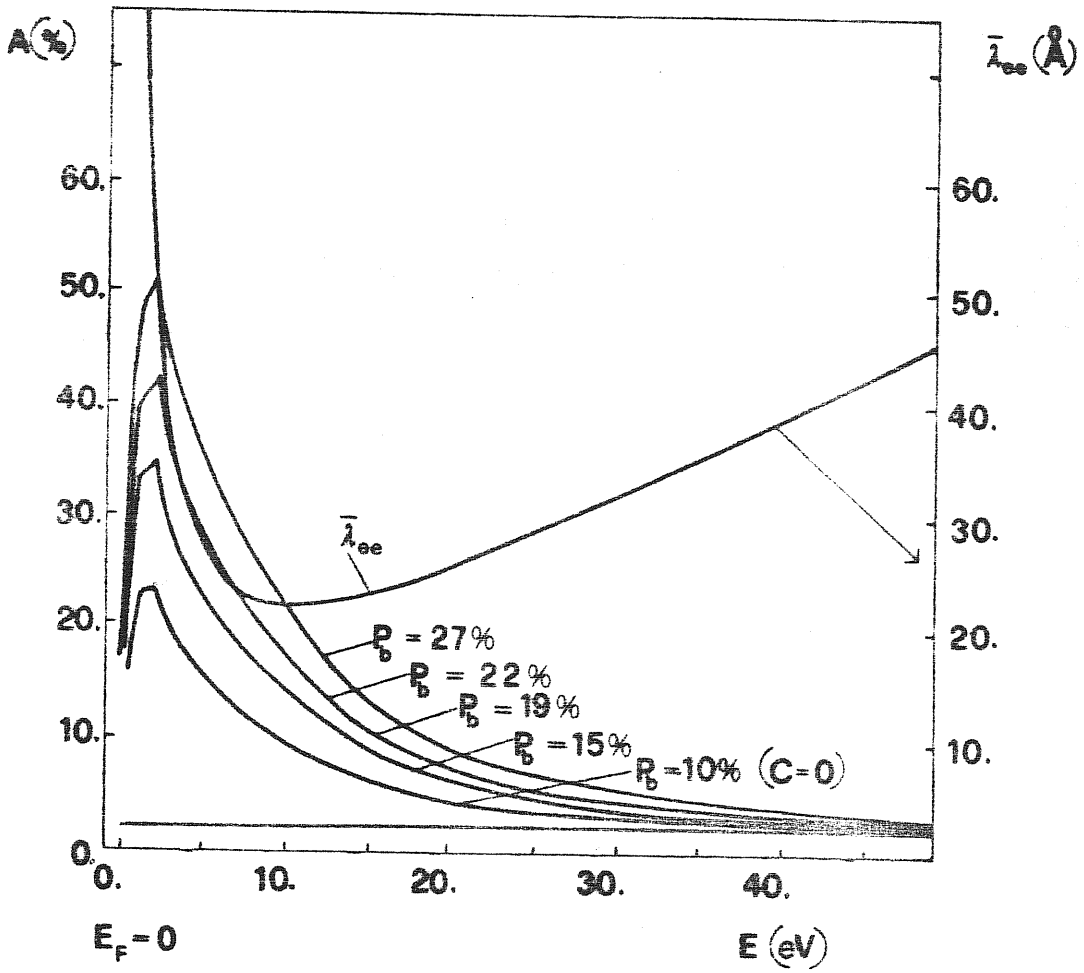

Fig.16

Average InMFP for e-e interaction $\bar{\lambda}_{ee}$, and asymmetry A between InMFP for up and down-spin electrons, for different bulk polarization as the functions of electron energy E.

P_b = 10% results from our model when c=0 , it means that all spin - asymmetry yields from "sp" splitting only. What we obtained is rather strong InMFP ; asymmetry peak (except for c=0) at $E=E_F+\Delta/2+\delta$ when electron energy coincides with empty $d^{\downarrow}$ - band. Note that it happens below the vacuum barrier (ϕ =4.3 eV). We display also the average e-e InMFP $\bar{\lambda}_{ee}$:

$$\bar{\lambda}_{ee} = \frac{1}{2}\left(\lambda_{ee}^{\uparrow} + \lambda_{ee}^{\downarrow}\right). \qquad (41)$$

Because of our neglect of many - body effects the minimum of $\bar{\lambda}_{ee}$ is shifted from ω_p to E_F. For the same reason the InMFP we obtained is larger than is expected , particularly for electron energies close and above ω_p .

The InMFP asymmetry A as presented on Fig. 16, particularly, the very small asymmetry for c = 0 , which is equivalent to complete quenching of our "d - bands", shows how crucial those bands are in determining the value of A.

To make this even clearer, we have calculated the asymmetry A for P_b = 22% (*i*) without d - (empty) band, and (*ii*) with both d - bands but without exchange interference term (negative terms in Eq.9 & 12b) which normally reduces interaction of parallel-spin electrons. (In this latter case the electron interactions become spin - independent and all spin effects occure only due to the difference between the majority and minority electronic density of states, occupied and empty).
We find (see Fig.17) that eliminating the d-bands (c=0)

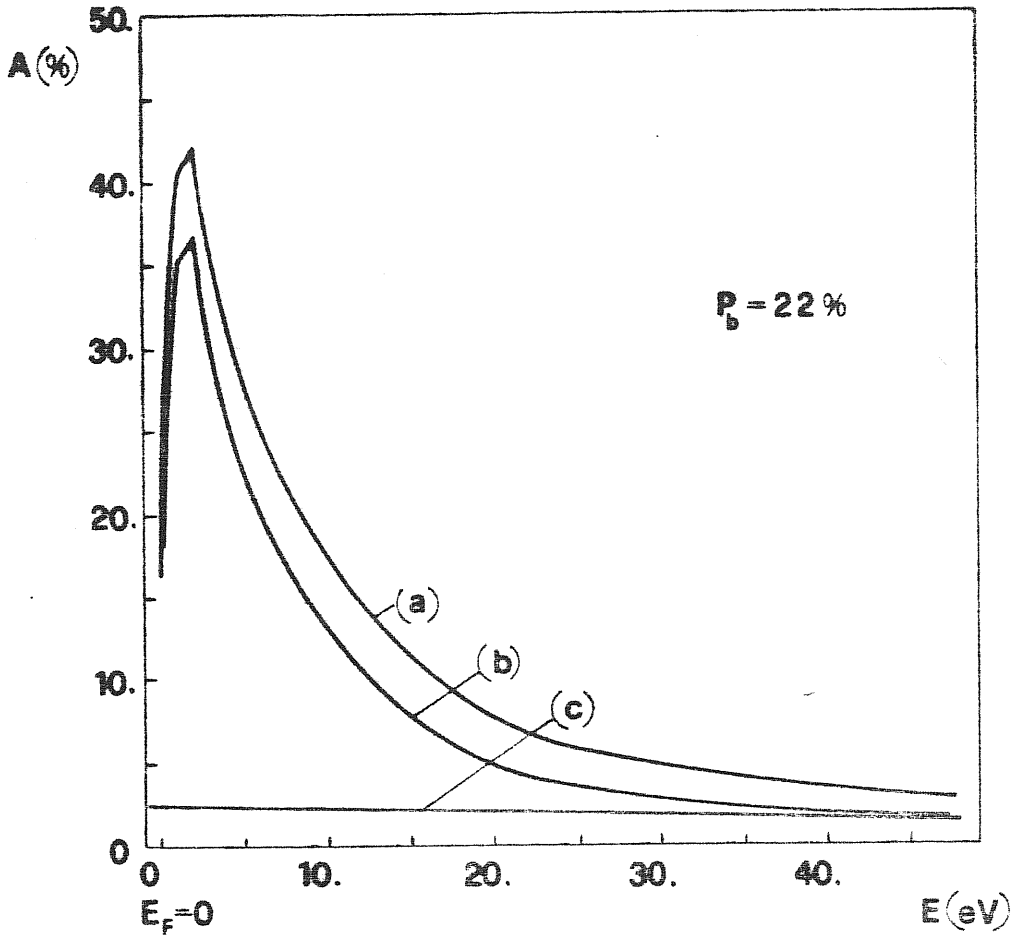

Fig.17

Inelastic mean-free-path asymmetry A for P_b=22%;
a) with both d-bands and with the exchange interference interaction between the parallel-spin electrons (the same curve as in Fig.16);
b) with both d-bands, but without exchange interference (spin-independent e-e interaction);
c) with exchange iterference, but without empty $d^{\downarrow}$-band.

reduces dramatically the asymmetry A , while on the other hand, even a spin-independent e-e interaction with d-band yields an asymmetry only slightly reduced with respect to the complete calculations. We conclude therefore, in agreement with the conjecture of Erskine & Stern [41], that the inelastic mean-free-path asymmetry A results mainly as an effect of the strong asymmetry between density of empty spin-up and spin-down states above the Fermi level. Having more empty states to fall down onto, that is, more chance to decay by emitting eventually a Stoner excitation (see Section 2), a spin-down electron has a larger probability of an energy loss than spin-up one. The spin-dependence of e-e interaction plays only minor role. In the work of Rendell & Penn [44] the spin-dependence of density of states above E_F was altogether ignored. In our opinion this is a reason for negative sign of A found by them for Fe and Co. The importance of spin-asymmetry in the densities of empty states has been already shown in spin-polarized photoelectron spectroscopy in Ni [45] and in Fe [46].

The asymmetry A which, we have obtained, exhibits a strong energy dependence. In particular, A decays rapidly with increasing electron energy. The explanation of this effect stems from simple phase - space considerations. The volume of the phase - space allowed for a decaying spin - up electron with energy E is roughly proportional to $E^{3/2}$. For spin - down electron this volume is proportional to $E^{3/2} + \mathcal{E}_d$, where $\mathcal{E}_d$ is the additional and constant contribution from the $d^{\downarrow}$-band. Thus, with E increasing the relative difference between phase-space

allowed for down and up-spin electrons, being proportional to $E^{-3/2}$, becomes smaller and smaller, and the InMFP asymmetry A decreases. Alternatively, but equivalently, one can just observe that the rate for creating Stoner excitations decreases for increasing energy.

The present calculations are limited only to Fe, but similar results, with smaller A value however, are expected for Co and Ni.

We do not know any experiment performed for the purpose of measuring the spin-dependence of InMFP (although the presence of an asymmetry A has of course an indirect impact on many experiments).

The direct observation of both average e-e InMFP $\bar{\lambda}_{ee}$ and its asymmetry A could be ideally performed by measurement of the polarization P_t of initially unpolarized electron beam, elastically transmitted through thin ferromagnetic film of thickness z. During that transission the fluxes of up and down spin electrons are diminished by factors $e^{-z/\lambda^{\uparrow}}$ and $e^{-z/\lambda^{\downarrow}}$ respectively, (here we neglect repeated elastic scattering),so polarization P_t is given by :

$$P_t = \frac{e^{-z/\lambda^{\uparrow}} - e^{-z/\lambda^{\downarrow}}}{e^{-z/\lambda^{\uparrow}} + e^{-z/\lambda^{\downarrow}}} , \qquad (42)$$

which, after some simple algebraical transformation turns out to be related to the asymmetry A in the form :

$$P_t = \tanh\left(z/\bar{\lambda}_{ee} \cdot \frac{A}{1-A^2}\right) , \qquad (43)$$

where $\bar{\lambda}_{ee}$ and A depend on electron energy. All other possible inelastic scattering mechanisms, if spin - independent , e.g. plasmon creation [26] , can not affect polarization P_t given by Eq. 43 since they reduce fluxes of both spins in the same way. Note also , that strongly depolarizing elastic - exchange scattering possible in paramagnets [47] , are suppressed in ferromagnets since spin - flip requires energy loss and is already accounted for in $\lambda_{ee}^{\uparrow(\downarrow)}$.

Pierce & Siegmann [48] have performed photoemission experiment with thin Ni films of various thic ness deposited on Cu substrate . The results of their measurements can be interpreted as induced by spin - dependence of In^{MFP} . However, both elastically and inelastically transmitted electrons have been observed simultaneously, while our considerations apply only to the elastically scattered . The authors of Ref.(48) avoid interpretations involving asymmetry of In^{MFP} (see also discussion in Ref.49).

We will now discuss briefly the possible influence of In^{MFP} asymmetry on photoemission experiments. This is important, since in presence of this asymmetry the polarization of photoexcited electrons could be altered while they travel through the ferromagnet, before escaping. To the extent to which this happens; it could then mask substantially he true initial band polarization one was trying to measure.

Suppose the photon beam of a given energy and intensity j_o , directed perpendicularly onto a ferromagnetic surface, penetrates the bulk of the solid exciting electrons with average spin - polarization P_{exc} . Let us denote by λ_{ph} the photon mean - free - path for that electron excitation. The probability for a photon

to reach the depth z is equal $e^{-z/\lambda_{ph}}$, the probability for the excitation of an up - spin electron in the interval $[\,z\,,\,z+dz\,]$ is equal: $\frac{\frac{1}{2}(1+P_{exc})}{\lambda_{ph}}\,dz$,

and the probability for the elastic escape of that electron is equal $e^{-z/\lambda^{\uparrow}}$ (for simplicity reason we consider here only the electrons drifting almost perpendicularly towards the surface). The electrons can be excited in any point along the photons path, so the intensity $j^{\uparrow}$ of elastically photoemited spin - up electrons is given by :

$$j^{\uparrow} = j_0 \frac{\frac{1}{2}(1+P_{exc})}{\lambda_{ph}} \int_0^{\infty} dz\, e^{-z/\lambda_{ph}}\, e^{-z/\lambda^{\uparrow}} \,, \qquad (44)$$

and after integration :

$$j^{\uparrow} = \frac{1}{2}\, j_0\, (1+P_{exc})\, \frac{\lambda^{\uparrow}}{\lambda_{ph}+\lambda^{\uparrow}} \,, \qquad (44a)$$

and the similar result for spin - down intensity :

$$j^{\downarrow} = \frac{1}{2}\, j_0\, (1-P_{exc})\, \frac{\lambda^{\downarrow}}{\lambda_{ph}+\lambda^{\downarrow}} \qquad (44b)$$

The spin - polarization of electrons leaving the solid P_{obs} is, as usually, given by:

$$P_{obs} = (j^{\uparrow} - j^{\downarrow}) / (j^{\uparrow} + j^{\downarrow}) .$$

The photon mean - free - path is much longer than the electron one : $\lambda_{ph} \gg \lambda^{\uparrow}, \lambda^{\downarrow}$. Within this limit P_{obs} is given by simple form :

$$P_{obs} = \frac{A + P_{exc}}{1 + P_{exc} \cdot A} , \qquad (45)$$

where InMFP asymmetry A depends on the electron energy. As seen from Fig. 16, for energetic electrons the difference between polarization measured outside the solid P_{obs} and that which electrons have just after excitation P_{exc} should be rather negligible. For low energy electrons , however, with energies about 10 eV or less , the excitation polarization can be quite different from that observed .

The interesting feature of Eq.45 should be noted : if $P_{exc} = \pm 100\%$, $P_{obs} = P_{exc}$ whatever value of A is. It means that spin - asymmetry of InMFP is <u>not</u> in contradiction with the possibility of the observation of -100% polarization of photoemitted electrons, as it is claimed for the photoemission from Ni [50] , if merely elastically photoemitted electrons are observed. The flux of elastic electrons decays exponentially , but the spins cannot be flipped without energy loss, so if only

spin - down electrons are excited , as it is reported in Ref. 50, the elastic electrons remain always completely down polarized.

We hope that the near future will bring new experimental results throwing more light on the spin-dependence of the InMFP of electrons in ferromagnets.

Acknowledgements

The author wish to express his gratitude to Prof. Erio Tosatti for pointing out interesting issues and for continuous support and interest on each stage of this thesis work.

This work has profited throughout from stimulating and informative discussions with M.Campagna, H.Hopster, M.Landolt and H.C.Siegmann. The author is also much indepted to Jülich and Zürich groups for informing him of their experimental results prior to publications.

APPENDIX

Analytical solution of simplified spin - polarized- - secondaries - cascade rate equations.

The goal of this Appendix is to give the analytical solution of the SPSEE rate equations of Section 3.1, with assumptions, made especially for this purpose, that will be clearly pointed out.

Let us rewrite Eq. 15 a & b assuming $R^{\uparrow\uparrow} = R^{\downarrow\downarrow}$, $R^{\uparrow\downarrow} = 0$, using dimensionless variables : $x = E/E_o$, $y = \omega/E_o$, and changing notation : $R^{\downarrow\uparrow} \to \alpha$, $R^{\uparrow\uparrow}$, $R^{\downarrow\downarrow} \to \beta$, $I^{\uparrow(\downarrow)} \to i^{\uparrow(\downarrow)}$:

$$\int_0^{1-x} dy \left[\beta(x+y, y)\, i^{\uparrow}(x+y) + \alpha(x+y, y)\, i^{\downarrow}(x+y)\right] + S = \int_0^{x} dy\, \beta(x,y)\, i^{\uparrow}(x) \quad , \qquad \text{(A1.a)}$$

$$\int_0^{1-x} dy \left[\beta(x+y, y)\, i^{\downarrow}(x+y) + S = \right.$$

$$= \int_0^{x} dy \left[\beta(x, y)\, i^{\downarrow}(x) + \alpha(x, y)\, i^{\downarrow}(x) \right., \qquad \text{(A1.b)}$$

where zero is on the Fermi level. The parameter s represents the source of electrons falling below energy E_o ($x = 1$) with constant and equal intensity for up and down spins. Introduction of s is more convenient for analytical solution than the boundary conditions used in 3.1.

We introduce further simplifying assumptions, namely:

$$\beta(x, y) \equiv \beta \quad , \qquad \text{(A2)}$$

$$\alpha(x, y) = \alpha\, \delta(y - 0) \quad . \qquad \text{(A3)}$$

Eq. A2 says that non - flip, or essentially direct scattering rate is independent of electron energy and of energy loss. In view of Fig.3, this is a very crude assumption, but not completely unrealistic. Eq.A3 sets to zero the energy loss for Stoner spin - flip process which is false in ferromagnetic iron, but makes the problem mathematically much more simpler. A solution with finite energy loss would not be much different. From Eqs. A1-A3 we have :

$$\alpha i^{\uparrow}(x) + \beta \int_{x}^{1} i^{\uparrow}(x')dx' - \beta x i^{\uparrow}(x) + S = 0 \quad , \tag{A4.a}$$

$$-\alpha i^{\downarrow}(x) + \beta \int_{x}^{1} i^{\downarrow}(x')dx' - \beta x i^{\downarrow}(x) + S = 0 \quad . \tag{A4.b}$$

We are looking for functions $i^{\uparrow}$ and $i^{\downarrow}$ for $0 < x < 1$.

The solution is straightford :

$$i^{\uparrow}(x) = \frac{S'(1+2\gamma)}{(1+\gamma)\,x^2} + \frac{2S'\gamma(1+\gamma)}{x^2}\left[\frac{\gamma}{2(x+\gamma)^2} + \right. \tag{A5}$$

$$\left. - \frac{1}{2(1+\gamma)^2} - \frac{1}{x+\gamma} + \frac{1}{1+\gamma}\right] ,$$

$$i^{\downarrow}(x) = \frac{S'(1+\gamma)}{(x+\gamma)^2} \quad , \tag{A6}$$

where $s' = s/\beta$ and $\gamma = \alpha/\beta$. It is easy to see that $\gamma < 1$; for the highest electron energy ($x = 1$) direct energy lóss has a probability $\beta \cdot 1$, which should be bigger than exchange probability α, hence, $\beta > \alpha$.

From Eq. A5 one can see the same $1/x^2$ increase for secondaries for decreasing energy as predicted e.g. in Ref.31. The singularity of i at zero energy (x=0) reflects the fact that electrons can not decay below Fermi level and they accumulate just there. (In numerical calculation in Section 3.1 we did not face that problem since we lost interest in all electrons fallen below the vacuum level).

For down spin electrons singularity vanishes (see Eq. A6), because down spin electrons have a possibility to turn to up ones by spin - flip process. Note that this drastic difference between $i^{\uparrow}$ and $i^{\downarrow}$ functions remains for any finite value of γ. However, there is always an energy range where exchange process, prevails upon direct process occuring with probability $\beta \cdot x$. This happens for x : $x < \gamma$. For those energies, the polarization P defined by Eq. 17 is approximately given by :

$$P \simeq 1 - 2x^2 \left(\frac{1+\gamma}{\gamma} \right)^2 , \qquad (A7)$$

which gives P = 100 % on Fermi level (x = 0).

As seen, the polarization enhancement is built up here only by exchange process set to be completely asymmetric. Of course, in reality the situation is much more complicated. (Our analytical solution is rather more akin to a gedanken experiment on a paramagnetic metal with spin-flip exchange process blocked for one spin direction).

Nevertheless that the very simple model solved

in this Appendix, gives a proper feeling of the mechanism of intensity and polarization growth of low energy SE , it also shows how a simple ideal spin-polarized electron cascade is characterized by a "critical"exponent" of 2, resulting by infinite repeated scattering.

REFERENCES

(1) L.Austin and H.Stark, Ann.Physik 9, 271 (1902)

(2) See for example A.J.Dekker,Solid State Physics Vol.6 Academic Press N.Y. (1958) and reference therein.

(3) P.Dirac, Proc.Roy.Soc. A 116, 227(1927)

(4) W.Pauli in "Le Magnetisme, Rapports et Discussions de Sixieme Conseil de Physique", Gauthier-Villars , Paris (1932)

(5) E.C.Stoner, Proc.Roy.Soc. A 165, 372(1938)

(6) N.F.Mott and H.S.W.Massey, "The theory of atomic collisions", Oxford Univ. Press 1965

(7) J.Kessler, "Polarized Electrons" Springer-Verlag Berlin Heidelberg, New York , 1976

(8) G.Busch, M.Campagna, P.Cotti and H.C.Siegmann Phys.Rev.Lett. 22, 597(1969)

(9) A.Bringer, M.Campagna, R.Feder, W.Gudat, E.Kisker and E.Kuhlman, Phys.Rev.Lett. 42, 1705 (1979)

(10) H.Raechter, in " Excitation of Plasmon and Interband Transition by Electrons " Vol.88 of Springs Tracts in Modern Physics, edited by H.Ralther (Springs, New York, 1980)

(11) H.Hopster, R.Raue and R.CLauberg , Phys.Rev.Lett. 53, 695 (1984)

(12) J.Kirschner, D.Rebenstorff and H.Ibach, Phys.Rev.Lett. 53, 698 (1984)

(13) J.Unguris, D.T.Pierce, A.Galejs and R.J.Cellotta Phys.Rev.Lett. 49, 72 (1982)

(14) E.Kisker, W.Gudat and K.Schröder, Solid State Comm. 44, 591 (1982)

(15) H.Hopster, R.Raue, E.Kisker, G.Günteherodt and M.Campagna, Phys.Rev.Lett. 50, 70 (1983)

(16) H.Hopster, private communication.

(17) J.Glazer, E.Tosatti, H.Hopster, R.Kurzawa, W.Schmitt, K.H.Walker and G.Güntherodt, to be published.

(18) S.Yin and E.Tosatti, ICTP preprint, IC/81/129 Trieste, (1981)

(19) J.Glazer, "Theory of Spin - Polarized Secondary Electron Emission", Magister Philosophiae thesis, International School for Advanced Studies , Trieste (1983), unpublished.

(20) J.Glazer and E.Tosatti, to be published.

(21) H.C.Siegmann, Int.School of Materials, Science and Technology, Ettore Majorana Centre, Erice (Italy) July,1984

(22) S.Modesti, R.Rosei, E.Tosatti, private communication.

(23) J.Callaway and C.S.Wang, Phys.Rev. B16, 2095 (1977)

(24) V.L.Moruzzi, J.F.Janak and A.R.Williams, "Calculated Electronic Properties of Metals", Pergamon Press, N.Y. Toronto etc., (1978)

(25) A.L.Fetter and J.D.Walecka "Quantum Theory of Many - Particles ", N.Y. McGraw-Hill, (1971)

(26) J.S.Helman and W.Beltensperger, Phys.Rev. B23, 1300 (1980).

(27) R.Rosei, private communication.

(28) H.Ibach and S.Lehwald, Solid State Comm. 45,633 (1983)

(29) R.F.Willis, B.Fitton and G.S.Painter, Phys.Rev. B9, 1926 (1974).

(30) M.S.Chung and T.E.Everhart, Phys.Rev. B15, 4699(1974)

(31) E.N.Sickafus, Surf.Sci., 100, 524 (1980) and references therein.

(32) J.P.Gauchaud and M.Cailler, Surf.Sci., 83, 498 & 519 (1979).

(33) S.Valkealahti and R.M.Nieminen, App.Phys. A, Springer - Verlag (1983).

(34) D.Mauri, Ph.D. thesis, Zürich (1983)

(35) J.B.Pendry, "Low - Energy Electron Diffraction", Oxford, Pergamon Press (1974).

(36) R.Feder. J.Phys. C14, 2049 (1981).

(37) J.Unguris, D.T.Pierce and R.J.Cellotta, Phys.Rev. B29, 1381 (1984).

(38) M.Landolt, private information.

(39) G.Ravano, E.Erbudak and H.C.Siegmann, Phys.Rev.Lett. 49, 80 (1982).

(40) J.A.D.Matthew, Phys.Rev. B25, 3326 (1982).

(41) J.L.Erskine and E.A.Stern, Phys.Rev.Lett. 30, 1329 (1973).

(42) H.C.Siegmann and M.Campagna, "Magnetism; Selected Topics", ed. by S.Foner, N.Y. Gordon and Breach , p.686 (1979).

(43) R.Feder, Solid State Comm. 31, 821 (1979).

(44) R.W.Rendell and David R.Penn, Phys.Rev.Lett. 45, 2057 (1980).

(45) J.Unguris, A.Seiber, R.J.Cellotta, D.T.Pierce , P.D.Johnson and N.V.Smith, Phys.Rev.Lett. 49, 1074 (1982).

(46) H.Scheidt, M.Glöbl, V.Dose and J.Kirschner , Phys.Rev.Lett. 51, 1688 (1983);

J.Kirschner, M.Glöbl, V.Dose and H.Scheidt , Phys.Rev.Lett. 53, 612 (1984).

(47) F.Meier, D.Pescia and M.Baumberger, Phys.Rev.Lett. 49, 747 (1982);

F.Meier, G.L.Bona and S.Hüfner, private communication.

(48) D.T.Pierce and H.C.Siegmann, Phys.Rev. B9, 4035 (1974).

(49) H.C.Siegmann, Phys.Reports 17C, 38 (1975).

(50) E.Kisker, W.Gudat, E.KUhlmann, R.Claberg and M.Campagna, Phys.Rev.Lett. 45, 2053, (1980).